

# Superposition of Quantum and Classical Rotational Motions in $\text{Sc}_2\text{C}_2@\text{C}_{84}$ Fullerite

K.H. Michel<sup>1</sup>, B. Verberck<sup>1</sup>, M. Hulman<sup>2,3</sup>, H. Kuzmany<sup>2</sup>, and M. Krause<sup>2,4</sup>

<sup>1</sup>*Departement Fysica, Universiteit Antwerpen,*

*Groenenborgerlaan 171, 2020 Antwerpen, Belgium*

<sup>2</sup>*Institut für Materialphysik der Universität Wien, Wien, Austria*

<sup>3</sup>*ARC Seibersdorf Research GmbH, A-2444 Seibersdorf, Austria*

<sup>4</sup>*Institute for Ion Beam Physics and Materials Research,*

*Forschungszentrum Rossendorf, PF510119, D-01314, Dresden, Germany*

(Dated: May 16, 2018)

## Abstract

The superposition of the quantum rotational motion (tunneling) of the encapsulated  $\text{Sc}_2\text{C}_2$  complex with the classical rotational motion of the surrounding  $\text{C}_{84}$  molecule in a powder crystal of  $\text{Sc}_2\text{C}_2@\text{C}_{84}$  fullerite is investigated by theory. Since the quantum rotor is dragged along by the  $\text{C}_{84}$  molecule, any detection method which couples to the quantum rotor (in casu the  $\text{C}_2$  bond of the  $\text{Sc}_2\text{C}_2$  complex) also probes the thermally excited classical motion (uniaxial rotational diffusion and stochastic meroaxial jumps) of the surrounding fullerene. The dynamic rotation-rotation response functions in frequency space are obtained as convolutions of quantum and classical dynamic correlation functions. The corresponding Raman scattering laws are derived, the overall shape of the spectra and the width of the resonance lines are studied as functions of temperature. The results of the theory are confronted with experimental low-frequency Raman spectra on powder crystals of  $\text{Sc}_2\text{C}_2@\text{C}_{84}$  [M. Krause et al., Phys. Rev. Lett. **93**, 137403 (2004)]. The agreement of theory with experiment is very satisfactory in a broad temperature range.

## I. INTRODUCTION

The existence of an endohedral fullerene, i.e. one or several atoms encapsulated in a fullerene molecule, was originally inferred from an analysis of mass spectra of  $\text{LaCl}_3$ -impregnated graphite and did lead to the proposal  $\text{La@C}_{60}$  [1]. At present the study of endohedral metallofullerenes  $\text{M}_x@\text{C}_n$ ,  $x = 1, 2, 3, 4$  and  $n = 66, 68, 72, 74, \dots, 100$ , where M are group II and III metals such as Sc, Y, ... or lanthanides Ce, ..., Lu, is a subject of interdisciplinary research [2] in physics, chemistry and materials sciences. By now one is able to produce materials where not only single atoms but clusters of atoms are encapsulated [3]. Due to charge transfer between the cluster and the surrounding carbon cage it is possible to obtain molecular-like complexes which do not exist otherwise (i.e. in absence of encapsulation) and which have unusual properties. Not only clusters with metal atoms of a same kind, such as the  $\text{Sc}_3$  trimer in  $\text{Sc}_3@\text{C}_{82}$  are produced, but also clusters composed of different kinds of atoms. A remarkable case is the production of  $\text{Sc}_2\text{C}_2@\text{C}_{84}$  in crystalline powder form [4]. The powder crystal is composed of crystallites where the  $\text{Sc}_2\text{C}_2@\text{C}_{84}$  units are arranged with average space group symmetry  $Fm\bar{3}m$ . From spectroscopic and structural characterization by NMR- and synchrotron X-ray diffraction experiments [4] it follows that the  $\text{Sc}_2\text{C}_2$  complex is encaged as a rigid unit with point group symmetry  $D_{2h}$  in a  $\text{C}_{84}$  fullerene of symmetry  $D_{2d}$  (isomer III, number 23 [5]). The center of mass of  $\text{Sc}_2\text{C}_2$  coincides with the center of mass of the molecule. The two Sc atoms are located at a distance of  $4.29(2)$  Å on the long  $C_2$  ( $S_4$ ) axis of  $\text{C}_{84}$ . The two C atoms of  $\text{Sc}_2\text{C}_2$  are located in the plane containing the two  $C_2$  axes perpendicular to the long axis of the  $\text{C}_{84}$  molecule and have a calculated distance of  $1.28$  Å. This distance lies between those of typical double and triple carbon bonds, and is consistent with the experimental and calculated C–C stretching frequency of the  $\text{C}_2$  unit (exp.  $1745$  cm $^{-1}$ , calc.  $1742$  cm $^{-1}$ ) [6]. In the following we will speak of this C–C bond as a  $\text{C}_2$  unit or molecule. Indeed low energy Raman spectra [6] on powder samples of  $\text{Sc}_2\text{C}_2@\text{C}_{84}$  in a temperature range  $25 - 150$  K (Kelvin) have revealed the existence of quantized rotational states of the  $\text{C}_2$  unit. The Raman lines' positions reflect transitions between energy levels of a  $\text{C}_2$  planar quantum rotor in a fourfold static potential due to the surrounding  $\text{C}_{84}$  cage. Therefore, one can speak of a quantum gyroscope.

In Ref. 6 the potential parameters of the encaged quantum rotor were obtained from density functional calculations using the VASP (Vienna ab initio simulation package) code

[7]. The energy levels were then determined from the solution of the Schrödinger equation. Within this approach, the Raman spectra consist of infinitely sharp lines while experimentally the lines are broadened and have a characteristic temperature behavior. A reason for this shortcoming is the restriction of the role of the encapsulating  $C_{84}$  molecule to a purely static body. Since the measured transition frequencies are in the range of  $10 - 80 \text{ cm}^{-1}$  and since the line broadening is of the order of a few  $\text{cm}^{-1}$ , any involvement of internal vibrational modes of the  $C_{84}$  cage as well as of stretching modes  $\text{Sc}-C_{84}$  can be excluded. The latter are of higher frequencies and have been measured in  $C_{84}$  and in  $\text{Sc}_2@C_{84}$  by infrared and Raman techniques [8, 9]. However the low-frequency external rotational modes of the  $C_{84}$  molecule and their superposition with the transitions of the quantum rotor should be retained: indeed the encapsulated  $\text{Sc}_2\text{C}_2$  gyroscope is dragged by the classical rotational motion of the  $C_{84}$  molecule and this dragging will affect the Raman spectrum of the  $C_2$  unit. It follows that an experimental probe such as Raman scattering which couples to the encapsulated species in an endohedral complex, in casu  $\text{Sc}_2\text{C}_2$ , also yields information on the dynamics of the encapsulating molecule, in casu  $C_{84}$ .

In the present paper we will extend the theoretical interpretation given in Ref. 6 and develop a unified theory where the quantum mechanical motion of the  $\text{Sc}_2\text{C}_2$  complex is coupled to the thermally excited classical rotational motion of the  $C_{84}$  fullerene. The coupling results from the fact that the long axis of the quantum gyroscope coincides with the  $S_4$  axis of the surrounding  $C_{84}$  molecule. In a given crystallite the  $C_{84}$  molecules are randomly oriented with their long  $C_2$  axis in equivalent  $\langle 100 \rangle$  directions of the face-centered cubic (fcc) unit cell [4]. We call this situation meroaxial disorder (this terminology seems to be more appropriate than merohedral disorder). We start from a model where at low temperature the meroaxially oriented  $C_{84}$  molecules in the fcc crystal perform uniaxial rotational diffusions about their long axis. Such a classical motion can be seen as a time-dependent modulation of the fourfold potential experienced by the quantum rotor and causes a temperature-dependent broadening of the quantum levels. An additional broadening effect is to be expected from the stochastic reorientations of the  $C_{84}$  molecules among the meroaxial directions which should become increasingly important at higher temperature. In addition, the stochastic reorientations lead to the appearance of a temperature-dependent quasi-elastic peak in the Raman spectrum.

The content of the paper is as follows. In Section II we write down the Raman scatter-

ing law for the  $C_2$ -unit belonging to the  $Sc_2C_2$  complex encapsulated by the  $C_{84}$  molecule in  $Sc_2C_2@C_{84}$  fullerite. We start from a single crystal with  $Fm\bar{3}m$  structure and static meroaxial disorder of the  $C_{84}$  molecules. Assuming a quantum mechanical rotational motion of the  $Sc_2C_2$  complexes and a classical rotational motion of the  $C_{84}$  molecules, the dynamic polarizability-polarizability correlation function is decoupled in a product of correlation functions for the rotational dynamics of  $Sc_2C_2$  and  $C_{84}$  respectively. The scattering law is obtained as a convolution of these correlation functions in Fourier space. Next (Sect. III) we calculate the correlation functions, using a quantum mechanical tunneling model for the  $Sc_2C_2$  complex and a uniaxial rotational diffusion model for the surrounding  $C_{84}$  molecule. The rotational diffusion motion of the encapsulating  $C_{84}$  molecule leads to a linear temperature-dependent broadening of the energy transition lines of the  $C_2$  planar rotor. In Sect. IV we extend the theory to a powder crystal which consists of arbitrarily oriented crystallites, each with  $Fm\bar{3}m$  space group symmetry and static meroaxial disorder. In the following (Sect. V) we consider the case of dynamic meroaxial disorder, describing the re-orientations of  $C_{84}$  molecules among the three meroaxial directions by a stochastic jump model. This model yields an exponential temperature-dependent broadening of the transition lines. In the last Section VI we give a numerical evaluation of the Raman scattering law for a  $Sc_2C_2@C_{84}$  powder crystal where quantum mechanical tunneling of the encapsulated  $Sc_2C_2$  units is superimposed by uniaxial rotational diffusion and dynamic meroaxial disorder of the  $C_{84}$  molecules. The temperature dependence of the line intensities and of the line broadenings is discussed.

## II. RAMAN SCATTERING LAW

We will derive the Raman scattering law where we limit ourselves to the interaction of the incident laser light with the plane rotational motion of the induced dipole of the C–C bond belonging to the  $Sc_2C_2$  complex of  $Sc_2C_2@C_{84}$ . This means that we consider the low frequency part of the spectrum (say  $\leq 100$   $cm^{-1}$ ). The  $Sc_2C_2$  complex is centered in the origin (center-of-mass position) of  $C_{84}$ . The long axis of  $Sc_2C_2$  coincides with the  $S_4$  axis of  $C_{84}$ . The C–C bond of  $Sc_2C_2$  lies in the plane containing the secondary  $C_2$  axes of  $C_{84}$  and rotates about the  $S_4$  axis. In that respect we will consider the C–C bond as a  $C_2$  planar rotor which experiences a fourfold potential inside the  $C_{84}$  molecule. Our formulation of

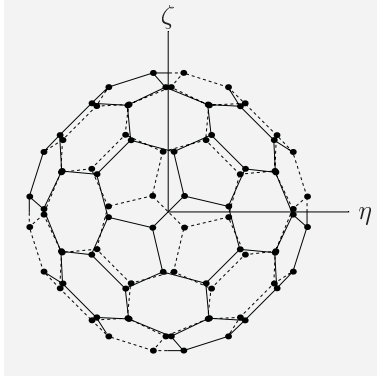


FIG. 1: View of the  $C_{84}$  molecule along the  $S_4$  axis.

the Raman scattering law is an extension of the conventional theory [10, 11] in as much as we describe a situation where the rotational motion of the induced dipole with respect to the laboratory-fixed frame is a superposition of the quantum motion of the  $C_2$  planar rotor inside the  $C_{84}$  molecule and of the classical motion of the  $C_{84}$  molecule in the laboratory frame.

We start with considering a single crystal of  $Sc_2C_2@C_{84}$  units with static meroaxial disorder. We assume that the  $Sc_2C_2@C_{84}$  units are statistically independent, hence it will be sufficient to consider one single representative unit. The cubic crystal axes ( $X', Y', Z'$ ) are chosen to coincide with the laboratory-fixed cubic coordinate system ( $X, Y, Z$ ). We consider a cubic system of axes ( $\xi, \eta, \zeta$ ) fixed in the  $C_{84}$  molecule such that the  $\xi$  axis coincides with the  $S_4$  axis while  $\eta$  and  $\zeta$  coincide with the secondary twofold axes (Fig. 1). The meroaxial orientations of the  $C_{84}$  molecules correspond to the situation where the  $\xi$  axes are randomly oriented along the  $X', Y'$  or  $Z'$  crystal axes. The  $C_2$  units then rotate in the planes ( $Y', Z'$ ), ( $Z', X'$ ) or ( $X', Y'$ ) respectively (Fig. 2). We say that the  $C_{84}$  molecule is in standard orientation if the  $S_4$  axis coincides with the laboratory-fixed  $X$  axis and the plane containing the secondary  $C_2$  axes coincides with the laboratory ( $Y, Z$ ) plane. The  $\zeta$  axis forms an angle  $\nu$  with the  $Z$  axis, while the C–C bond forms an angle  $\tau$  with the  $\zeta$  axis. Hence the polar angle  $\theta$  of the C–C bond with the laboratory  $Z$  axis (Fig. 3) is a sum of two terms:

$$\theta = \nu + \tau. \quad (2.1)$$

Since the  $C_2$  rotor is confined to the ( $Y, Z$ ) plane, the azimuthal angle  $\phi$  measured away from  $X$  has value  $\pi/2$ . The distinction of two contributions to the angle  $\theta$  is essential.

In the following we will assign the angular variable  $\tau$  to the quantum mechanical tunneling

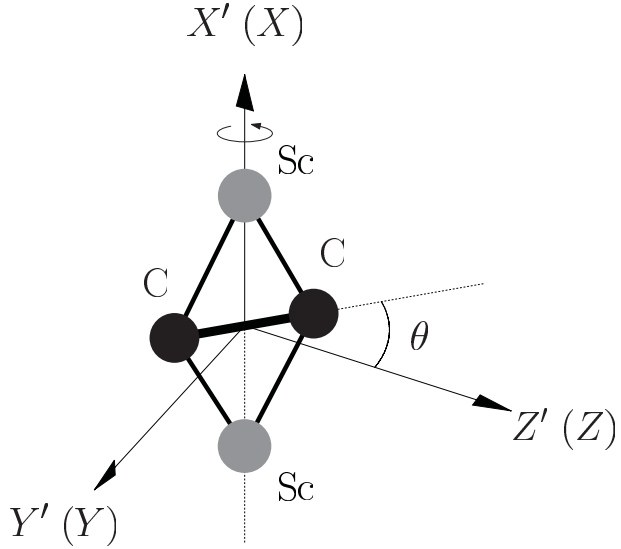


FIG. 2: The  $\text{Sc}_2\text{C}_2$  complex in the crystal-fixed cubic coordinate system  $(X', Y', Z')$  while the  $\text{C}_{84}$  molecule is in standard orientation.

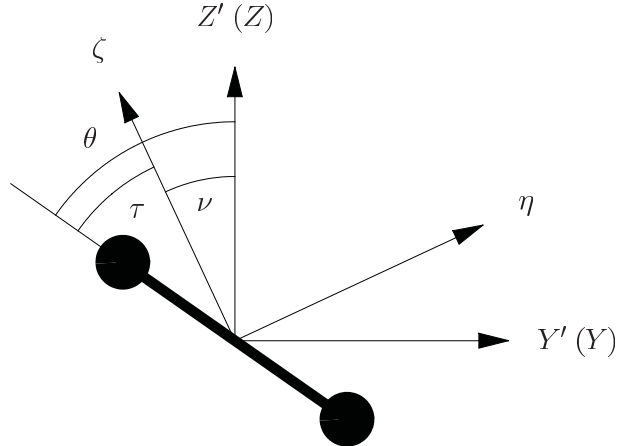


FIG. 3: Orientation of the  $\text{C}_2$  bond of  $\text{Sc}_2\text{C}_2$  in the rotatory reflection plane of the  $\text{C}_{84}$  molecule ( $\text{C}_{84}$  in standard orientation).

of the  $\text{Sc}_2\text{C}_2$  complex about its long axis inside the  $\text{C}_{84}$  cage and the angular variable  $\nu$  to the thermally excited classical rotation of the  $\text{C}_{84}$  molecule about the  $S_4$  axis. The assumption of classical uniaxial rotational diffusion motion as a first approximation to the dynamics of the  $\text{C}_{84}$  molecule at low temperature is motivated by the structural results of meroaxial disorder [4]. It is also inspired from the dynamics of solid  $\text{C}_{70}$  in the rhombohedral and monoclinic phases. There the importance of uniaxial rotational diffusion about the long axis of the  $\text{C}_{70}$  molecule has been probed by muon spin spectroscopy [12, 13], nuclear magnetic resonance

[14, 15, 16] and inelastic neutron scattering [17].

We treat the C–C bond of  $\text{Sc}_2\text{C}_2$  as a rigid cylindrical rod with longitudinal and transverse static polarizability  $\alpha_{\parallel}$  and  $\alpha_{\perp}$  respectively. The Raman scattering law for incident and scattered radiation in  $Z$  direction is given by the Fourier transform of the time-dependent autocorrelation function of the polarizability  $\alpha_{ZZ}$ :

$$R_{ZZZZ}(\omega) = \frac{N}{2\pi} \int_{-\infty}^{+\infty} dt e^{i\omega t} \langle \alpha_{ZZ}(t) \alpha_{ZZ}(0) \rangle. \quad (2.2)$$

Here  $N$  is the number of  $\text{Sc}_2\text{C}_2@\text{C}_{84}$  units and  $\omega$  is the frequency difference of incident and scattered radiation. The polarizability has to be understood as an average over the three meroaxial molecular orientations. In the following we label these orientations by a superscript  $(i)$ ,  $i = 1, 2, 3$ . If the  $\text{C}_{84}$  molecule is in standard orientation ( $\xi$  axis  $\parallel X$ ), or in orientation  $\xi \parallel Y$ , the corresponding orientation-dependent polarizabilities  $\alpha_{ZZ}^{(1)}$  and  $\alpha_{ZZ}^{(2)}$  are equal and given by [10]

$$\alpha_{ZZ}^{(1)} = \alpha_{ZZ}^{(2)} = \frac{\alpha_{\perp} + \alpha_{\parallel}}{2} + \frac{\alpha_{\parallel} - \alpha_{\perp}}{2} \cos 2\theta, \quad (2.3)$$

while with  $\xi \parallel Z$  one has

$$\alpha_{ZZ}^{(3)} = \alpha_{\perp}, \quad (2.4)$$

independent of  $\theta$ . In the case of meroaxial disorder, the average polarizability is given by

$$\alpha_{ZZ} = \frac{1}{3} \sum_{i=1}^3 \alpha_{ZZ}^{(i)} = a + \frac{2}{3} b \cos 2\theta \quad (2.5)$$

where we have defined

$$a = \frac{\alpha_{\parallel} + 2\alpha_{\perp}}{3}, \quad b = \frac{\alpha_{\parallel} - \alpha_{\perp}}{2}. \quad (2.6)$$

Hence the time-dependent correlation function reads

$$\langle \alpha_{ZZ}(t) \alpha_{ZZ}(0) \rangle = a^2 + \frac{4b^2}{9} \langle \cos 2\theta(t) \cos 2\theta(0) \rangle. \quad (2.7)$$

Similarly we obtain for incident radiation in  $Z$  direction and scattered radiation in  $Y$  direction

$$R_{ZYZY}(\omega) = \frac{N}{2\pi} \int_{-\infty}^{+\infty} dt e^{i\omega t} \langle \alpha_{ZY}(t) \alpha_{ZY}(0) \rangle. \quad (2.8)$$

If the  $C_{84}$  molecule is in standard orientation,

$$\alpha_{ZY}^{(1)} = b \sin 2\theta, \quad (2.9)$$

while for  $\xi \parallel Y$ ,  $\alpha_{ZY}^{(2)} = 0$ , and  $\xi \parallel Z$ ,  $\alpha_{ZY}^{(3)} = 0$ . The average polarizability for the case of meroaxial disorder reads

$$\alpha_{ZY} = \frac{b}{3} \sin 2\theta, \quad (2.10)$$

and the correlation function becomes

$$\langle \alpha_{ZY}(t) \alpha_{ZY}(0) \rangle = \frac{b^2}{9} \langle \sin 2\theta(t) \sin 2\theta(0) \rangle. \quad (2.11)$$

The problem of determining the scattering laws  $R_{ZZZZ}(\omega)$  and  $R_{ZYZY}(\omega)$  consists in the calculation of the orientation-orientation thermal correlation functions

$$C(t) = \langle \cos 2\theta(t) \cos 2\theta(0) \rangle, \quad (2.12)$$

$$S(t) = \langle \sin 2\theta(t) \sin 2\theta(0) \rangle, \quad (2.13)$$

Taking into account the basic relation Eq. (2.1), we expand in terms of  $\cos 2\tau$ ,  $\sin 2\tau$ ,  $\cos 2\nu$  and  $\sin 2\nu$  thereby obtaining correlation functions of the form

$$C^{cccc}(t) = \langle \cos 2\tau(t) \cos 2\nu(t) \cos 2\tau(0) \cos 2\nu(0) \rangle, \quad (2.14)$$

$$S^{cscs}(t) = \langle \cos 2\tau(t) \sin 2\nu(t) \cos 2\tau(0) \sin 2\nu(0) \rangle, \quad (2.15)$$

and similarly for  $C^{ssss}(t)$  and  $S^{scsc}(t)$ . Observing that  $\tau$  refers to quantum dynamics of  $C_2$  and  $\nu$  to classical dynamics of  $C_{84}$ , we decouple the thermal averages:

$$C^{cccc} = Q^{cc}(t) F^{cc}(t), \quad C^{ssss} = Q^{ss}(t) F^{ss}(t), \quad (2.16)$$

$$S^{cscs} = Q^{cc}(t) F^{ss}(t), \quad S^{scsc} = Q^{ss}(t) F^{cc}(t). \quad (2.17)$$

Here the correlation functions

$$Q^{cc}(t) = \langle \cos 2\tau(t) \cos 2\tau(0) \rangle, \quad (2.18)$$

$$Q^{ss}(t) = \langle \sin 2\tau(t) \sin 2\tau(0) \rangle, \quad (2.19)$$

describe the quantum dynamics of the  $C_2$  unit while the correlation functions

$$F^{cc}(t) = \langle \cos 2\nu(t) \cos 2\nu(0) \rangle, \quad (2.20)$$

$$F^{ss}(t) = \langle \sin 2\nu(t) \sin 2\nu(0) \rangle, \quad (2.21)$$

describe the classical dynamics of the surrounding  $C_{84}$  molecule. Finally quantum and classical dynamics occur as products of correlation functions:

$$C(t) = Q^{cc}(t)F^{cc}(t) + Q^{ss}(t)F^{ss}(t), \quad (2.22)$$

$$S(t) = Q^{ss}(t)F^{cc}(t) + Q^{cc}(t)F^{ss}(t). \quad (2.23)$$

Defining Fourier transforms

$$Q(\omega) = \frac{1}{2\pi} \int_{-\infty}^{+\infty} dt e^{i\omega t} Q(t), \quad (2.24)$$

$$F(\omega) = \frac{1}{2\pi} \int_{-\infty}^{+\infty} dt e^{i\omega t} F(t), \quad (2.25)$$

and using Eqs. (2.22), (2.23), (2.7) and (2.11), we rewrite the Raman scattering law in terms of convolutions of Fourier-transformed quantum and classical correlation functions, thereby obtaining

$$R_{ZZZZ}(\omega) = N \left[ a^2 \delta(\omega) + \frac{4b^2}{9} C(\omega) \right], \quad (2.26)$$

with scattering function

$$C(\omega) = \int_{-\infty}^{+\infty} d\omega' [Q^{cc}(\omega - \omega')F^{cc}(\omega') + Q^{ss}(\omega - \omega')F^{ss}(\omega')], \quad (2.27)$$

and

$$R_{ZYZY}(\omega) = N \frac{b^2}{9} S(\omega), \quad (2.28)$$

with scattering function

$$S(\omega) = \int_{-\infty}^{+\infty} d\omega' [Q^{ss}(\omega - \omega')F^{cc}(\omega') + Q^{cc}(\omega - \omega')F^{ss}(\omega')]. \quad (2.29)$$

The first term in brackets on the right-hand side of Eq. (2.26) corresponds to the unshifted Rayleigh line of the spectrum while the function  $C(\omega)$  (as also  $S(\omega)$  in Eq. (2.28)) accounts for the inelastic part. Expressions (2.27) and (2.29) which are convolutions in Fourier space show that the quantum motion of the  $C_2$  rotor is modulated by the classical rotational motion of the surrounding  $C_{84}$  cage. This is an example of “direct coupling” of two motions through the detection process [18], in contradistinction to the “indirect coupling” through a Hamiltonian. The origin of the direct coupling here is due to the fact that the detection angle  $\theta$  is a sum of two terms, Eq. (2.1).

In the next section we will calculate the quantum mechanical and classical orientational correlation functions for  $C_2$  and  $C_{84}$  respectively.

### III. DYNAMIC CORRELATIONS

#### A. $C_2$ quantum rotor

The quantum mechanics of a diatomic molecular rotor in crystals goes back to Pauling [19]. A still valid review of the subject of single particle rotations in molecular crystals has been given by W. Press [20]. We will calculate the orientational autocorrelation functions  $Q^{cc}$  and  $Q^{ss}$  by starting from the model of the  $C_2$  planar quantum rotor in the fourfold potential due to the  $C_{84}$  cage. We will refer to this motion as rotational tunneling [20, 21]. We will show that the resonances of the correlation functions  $Q^{cc}(\omega)$  and  $Q^{ss}(\omega)$  are due to transitions between tunneling energy levels. The sole degree of freedom is the angle  $\tau$  which accounts for the rotatory motion of  $C_2$  with respect to the cage. The corresponding Schrödinger equation reads

$$\left[ -B \frac{d^2}{d\tau^2} + \frac{V_0}{2} (1 - 4 \cos 4\tau) \right] \psi(\tau) = E \psi(\tau). \quad (3.1)$$

Here  $B = \hbar^2/2I$  is the rotational constant and  $I$  the moment of inertia of  $C_2$ ,  $V_0$  is the barrier height of the potential. The rotational constant has the dimension of an energy, from experiment [6] one deduces  $B = 1.73 \text{ cm}^{-1}$  (wave number units) and  $V_0 = 8B$ . These values are supported by ab initio density functional calculations [6]. Equation (3.1) which is an extension of Mathieu's equation [19, 22] is also called Hill's equation [23]. With the definitions

$$\alpha = \frac{1}{B} \left( E - \frac{V_0}{2} \right), \quad q = \frac{V_0}{4B}, \quad (3.2)$$

Eq. (3.1) reads

$$\left[ \frac{d^2}{d\tau^2} + \alpha + 2q \cos 4\tau \right] \psi(\tau) = 0. \quad (3.3)$$

From symmetry considerations (nuclear spin is zero for  $^{12}\text{C}$ , electron wave function of  $C_2^2$  is totally symmetric), it follows that the rotational wave function  $\psi(\tau)$  must be symmetric with respect to the operation  $\tau \rightarrow \tau - \pi$ . For even periodic solutions one makes the ansatz

$$\psi^+(\tau) = \sum_{m=0}^{\infty} A_{2m} \cos(2m\tau), \quad (3.4)$$

$m = 0, 1, 2, \dots$ . Equation (3.3) then leads to an infinite system of homogeneous equations for the coefficients  $A_{2m}$ . Truncation of this system for a given value  $m = N$  leads to  $N + 1$

equations which separate into two systems: a first one for  $\{A_0, A_4, \dots, A_{2N}\}$  and a second one for  $\{A_2, A_6, \dots, A_{2N-2}\}$  (we take  $N$  even). Solving for the two discriminants yields the roots  $\alpha_{2m}^+(q)$  for  $m = 0, 2, \dots, N$  and  $m = 1, 3, \dots, N-1$ . In case of zero potential, i.e.  $q = 0$ , these solutions reduce to the free planar rotor energies  $\{E_{2m}^+(q = 0)\} = \{0, \dots, (2m)^2 B, \dots\}$  with normalized eigenfunctions

$$\{\psi_{2m}^+(\tau)\} = \left\{ \frac{1}{\sqrt{\pi}}, \dots, \frac{\cos(2m\tau)}{\sqrt{\pi/2}}, \dots \right\} \quad (3.5)$$

in the interval  $0 \leq \tau \leq \pi$ . The ansatz for odd periodic solutions reads

$$\psi^-(\tau) = \sum_{m=1}^{\infty} B_{2m} \sin(2m\tau). \quad (3.6)$$

Proceeding as before one determines the roots  $\alpha_{2m}^-(q)$ . In case of zero potential the eigenfunctions are

$$\{\psi_{2m}^-(\tau)\} = \left\{ \frac{\sin 2\tau}{\sqrt{\pi}}, \dots, \frac{\sin(2m\tau)}{\sqrt{\pi/2}}, \dots \right\}. \quad (3.7)$$

In the following we will label the energy eigenfunctions and eigenvalues by the double index  $(\sigma, 2m)$ ,  $\sigma = \pm$ , also in the case of nonzero potential. In Fig. 4 we show plots of  $\frac{E_{2m}^\sigma(q)}{B} = \alpha_{2m}^\sigma(q) + 2q$ .

We next perform a spectral decomposition of the correlation functions  $Q^{\text{cc}}(t)$  and  $Q^{\text{ss}}(t)$  in terms of eigenfunctions and eigenvalues of the Schrödinger equation (3.1). In general form the result reads

$$Q^{\text{cc}}(t) = \frac{1}{Z} \sum_{i,j} e^{-E_i/T} |C_{ij}|^2 e^{i(E_i - E_j)t/\hbar}, \quad (3.8)$$

$$Q^{\text{ss}}(t) = \frac{1}{Z} \sum_{i,j} e^{-E_i/T} |S_{ij}|^2 e^{i(E_i - E_j)t/\hbar}, \quad (3.9)$$

where

$$C_{ij} = \langle i | \cos 2\tau | j \rangle, \quad (3.10)$$

$$S_{ij} = \langle i | \sin 2\tau | j \rangle. \quad (3.11)$$

Here the label  $i$  ( $j$ ) stands for the double index  $(\sigma, 2m)$  of the solutions of the Schrödinger equation. We calculate the matrix elements  $C_{ij}$  and  $S_{ij}$  with the free planar rotor energies.

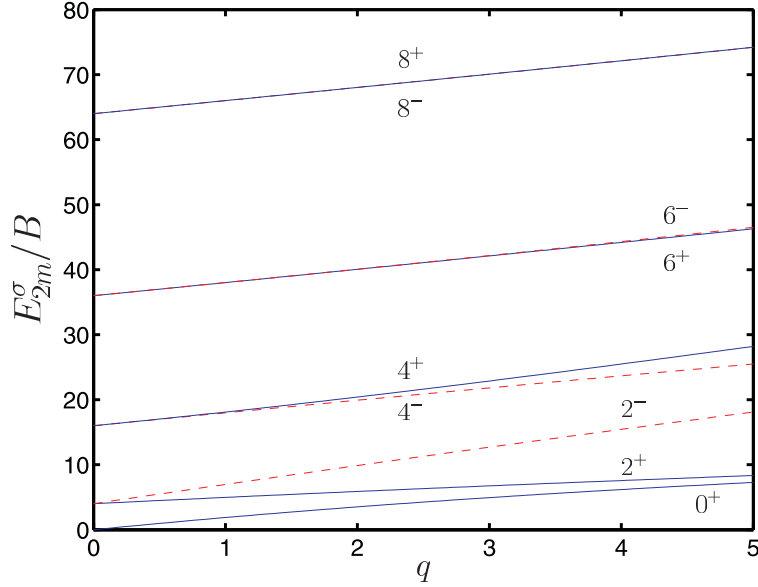


FIG. 4: Energy levels of the  $C_2$  planar quantum rotor in the fourfold molecular potential as a function of the potential strength  $q$  (dimensionless units). Only levels up to  $2m = 8$  are shown.

Symmetry implies that only functions of a same parity  $(+, +)$  or  $(-, -)$  contribute to  $C_{ij}$  while  $S_{ij}$  differs from zero only for functions  $i, j$  with different parity. For instance

$$C_{2m2n}^{++} = \int_0^\pi d\tau \frac{\cos(2m\tau)}{\sqrt{\pi/2}} \cos 2\tau \frac{\cos(2n\tau)}{\sqrt{\pi/2}} = \frac{1}{2} \delta_{m,n\pm 1}, \quad (3.12)$$

$$S_{2m2n}^{+-} = \int_0^\pi d\tau \frac{\cos(2m\tau)}{\sqrt{\pi/2}} \sin 2\tau \frac{\sin(2n\tau)}{\sqrt{\pi/2}} = \frac{1}{2} \delta_{m,n\pm 1}, \quad (3.13)$$

These matrix elements imply selection rules for transitions between energy levels. We take Fourier transforms of Eqs. (3.8) and (3.9), using the identity

$$\frac{1}{2\pi} \int_{-\infty}^{+\infty} dt e^{i\omega t} e^{i(E_i - E_j)t/\hbar} = \delta \left( \omega - \left( \frac{E_j - E_i}{\hbar} \right) \right). \quad (3.14)$$

We insert the energies

$$E_{2m}^\sigma = B\alpha_{2m}^\sigma(q) + \frac{V_0}{2}, \quad (3.15)$$

and take into account the selection rules (3.12) – (3.13). Defining the frequency transfer

$$\omega_{mn}^{\sigma\sigma'} = \frac{E_{2n}^{\sigma'} - E_{2m}^\sigma}{\hbar}, \quad (3.16)$$

we obtain

$$Q^{cc}(\omega) = \frac{1}{2Z} \left\{ e^{-E_0^+/T} \delta(\omega - \omega_{01}^{++}) + \sum_{m=1}^{\infty} \frac{e^{-E_{2m}^+/T}}{2} [\delta(\omega - \omega_{mm+1}^{++}) + \delta(\omega - \omega_{mm-1}^{++})] \right. \\ \left. + \frac{e^{-E_2^-/T}}{2} [\delta(\omega - \omega_{12}^{--}) + \sum_{m=2}^{\infty} \frac{e^{-E_{2m}^-/T}}{2} [\delta(\omega - \omega_{mm+1}^{--}) + \delta(\omega - \omega_{mm-1}^{--})]] \right\}, \quad (3.17)$$

with

$$Z = e^{-E_0^+/T} + \sum_{m=1}^{\infty} \left( e^{-E_{2m}^+/T} + e^{-E_{2m}^-/T} \right). \quad (3.18)$$

Similarly we get

$$Q^{ss}(\omega) = \frac{1}{2Z} \left\{ e^{-E_0^+/T} \delta(\omega - \omega_{01}^{+-}) \right. \\ \left. + \frac{e^{-E_2^+/T}}{2} \delta(\omega - \omega_{12}^{+-}) + \sum_{m=2}^{\infty} \frac{e^{-E_{2m}^+/T}}{2} [\delta(\omega - \omega_{mm+1}^{+-}) + \delta(\omega - \omega_{mm-1}^{+-})] \right. \\ \left. + \sum_{m=1}^{\infty} \frac{e^{-E_{2m}^-/T}}{2} [\delta(\omega - \omega_{mm+1}^{-+}) + \delta(\omega - \omega_{mm-1}^{-+})] \right\}. \quad (3.19)$$

We notice that in absence of the uniaxial rotation of the  $C_{84}$  cage, i.e. for  $\nu = 0$ , the correlation functions Eqs. (2.20) and (2.21) reduce to constants:  $F^{cc} = 1$ ,  $F^{ss} = 0$ . Hence the spectral functions  $C(\omega)$  and  $S(\omega)$  entering the Raman scattering laws Eqs. (2.26) and (2.28) reduce to  $Q^{cc}(\omega)$  and  $Q^{ss}(\omega)$  and exhibit infinitely sharp  $\delta$ -peaks which account for transitions between quantized planar rotor states. In Table I we have quoted some values ( $m \leq 4$ ) of  $\omega_{mn}^{\sigma\sigma'}$  for  $q = 0$  (free rotor) and  $q = 2$  (value of the potential strength taken from experiment in Ref. 6).

## B. $C_{84}$ uniaxial rotational diffusion

In order to calculate the classical correlation functions  $F^{cc}(t)$  and  $F^{ss}(t)$  we treat the  $C_{84}$  molecule as a classical uniaxially diffusing rotor with rotation axis  $S_4$  in coincidence with a cubic crystal axis, in casu the  $X'$  axis. The corresponding rotation angle  $\nu$  is measured away from the  $Z'$  axis. Equivalently one considers the  $S_4$  axis along  $Y'$  and  $Z'$  (meroaxial disorder). Given the  $S_4$  axis it would be tempting to study this motion in a crystal field potential of fourfold symmetry. Such a study can be carried out along the lines of Ref. 24 and leads to a continued fraction expansion in terms of frequency moments of the orientational

TABLE I: Tunneling frequency transfers  $\omega_{mn}^{\sigma\sigma'}$ ,  $n = m \pm 1$ ,  $\sigma, \sigma' = \pm$ , in units  $\text{cm}^{-1}$ .

$m$	$\omega_{mm+1}^{++}$	$\omega_{mm+1}^{--}$	$\omega_{mm+1}^{+-}$	$\omega_{mm+1}^{-+}$	$\omega_{mm-1}^{++}$	$\omega_{mm-1}^{--}$	$\omega_{mm-1}^{+-}$	$\omega_{mm-1}^{-+}$
$q = 0$								
0	6.92		6.92					
1	20.76	20.76	20.76	20.76	-6.92			-6.92
2	34.60	34.60	34.60	34.60	-20.76	-20.76	-20.76	-20.76
3	48.44	48.44	48.44	48.44	-34.60	-34.60	-34.60	-34.60
4	62.28	62.28	62.28	62.28	-48.44	-48.44	-48.44	-48.44
$q = 2$								
0	4.10		10.99					
1	25.12	17.39	24.28	18.23	-4.10			-10.99
2	34.00	34.87	34.02	34.84	-25.12	-17.39	-18.23	-24.28
3	48.40	48.38	48.40	48.38	-34.00	-34.87	-34.84	-34.02
4	62.26	62.26	62.26	62.26	-48.40	-48.38	-48.38	-48.40

variables. It is adequate in the case of a strong crystal field potential since then one can limit the continued fraction to a few steps. However this approximation is not valid in the case of weak potentials. Since the equator of the  $\text{C}_{84}$  molecule for rotations about  $S_4$  deviates only slightly from circular shape, we prefer to consider the rotator about the  $S_4$  axis in the rotational-diffusion approximation. This model has the obvious advantage of simplicity and leads to a linear temperature-dependent broadening of the tunneling transition lines. Within the uniaxial diffusion model the  $\text{C}_{84}$  molecule experiences a random rotational torque (also called Brownian motion torque) about its  $S_4$  axis. This torque is caused by the thermal motion of the surrounding lattice (heat bath). In that respect the present problem is different from the situation of the heavy symmetrical top with gravitational torque since on the molecular scale the effect of gravitation is negligible in comparison with the heat bath.

The idea of rotational diffusion goes back to Debye [25] who applied the concept of rotational Brownian motion to the theory of dielectric relaxation (see also [20] and [26]). In

Appendix A we give some details for the present problem. As a result we obtain

$$F^{cc}(t) = \langle \cos 2\nu(t) \cos 2\nu(0) \rangle = \frac{1}{2} e^{-4D_R t}, \quad (3.20)$$

$$F^{ss}(t) = \langle \sin 2\nu(t) \sin 2\nu(0) \rangle = \frac{1}{2} e^{-4D_R t}. \quad (3.21)$$

Here the rotational diffusion coefficient  $D_R$  is given by the Einstein relation

$$D_R = \frac{k_B T}{\zeta}, \quad (3.22)$$

where  $\zeta$  is the friction coefficient and  $T$  the temperature. The equality of  $F^{cc}(t)$  and  $F^{ss}(t)$  is a consequence of our neglect of the crystal field potential within the large-friction approximation. From Eqs. (2.22) and (2.23) one sees that then

$$C(t) = S(t). \quad (3.23)$$

In the following we will neglect the superscripts  $ss$  and  $cc$  on  $F^{cc}$  and  $F^{ss}$  and write just  $F$ .

The Fourier transform is obtained from Eq. (3.21) with the result

$$F(\omega) = \frac{1}{2\pi} \left[ \frac{4D_R}{\omega^2 + 16D_R^2} \right]. \quad (3.24)$$

We rewrite the scattering functions Eqs. (2.27) and (2.29) as

$$C(\omega) = S(\omega) = \int_{-\infty}^{+\infty} d\omega' [Q^{ss}(\omega - \omega') + Q^{cc}(\omega - \omega')] F(\omega'). \quad (3.25)$$

Using expressions (3.17) and (3.19) we carry out the integral over  $\omega'$  and obtain

$$C(\omega) = C_{++}(\omega) + C_{--}(\omega) + C_{+-}(\omega) + C_{-+}(\omega) \quad (3.26)$$

where

$$C_{++}(\omega) = \frac{1}{2Z} \left\{ e^{-E_0^+/T} F(\omega - \omega_{01}^{++}) + \sum_{m=1}^{\infty} \frac{e^{-E_{2m}^+/T}}{2} [F(\omega - \omega_{mm+1}^{++}) + F(\omega - \omega_{mm-1}^{++})] \right\}, \quad (3.27)$$

$$C_{--}(\omega) = \frac{1}{2Z} \left\{ \frac{e^{-E_2^-/T}}{2} F(\omega - \omega_{12}^{--}) + \sum_{m=2}^{\infty} \frac{e^{-E_{2m}^-/T}}{2} [F(\omega - \omega_{mm+1}^{--}) + F(\omega - \omega_{mm-1}^{--})] \right\}, \quad (3.28)$$

$$C_{+-}(\omega) = \frac{1}{2Z} \left\{ e^{-E_0^+/T} F(\omega - \omega_{01}^{+-}) + \frac{e^{-E_2^+/T}}{2} F(\omega - \omega_{12}^{+-}) + \sum_{m=2}^{\infty} \frac{e^{-E_{2m}^+/T}}{2} [F(\omega - \omega_{mm+1}^{+-}) + F(\omega - \omega_{mm-1}^{+-})] \right\}, \quad (3.29)$$

$$C_{-+}(\omega) = \frac{1}{2Z} \left\{ \sum_{m=1}^{\infty} \frac{e^{-E_{2m}^-/T}}{2} [F(\omega - \omega_{mm+1}^{-+}) + F(\omega - \omega_{mm-1}^{-+})] \right\}. \quad (3.30)$$

We see that  $C(\omega)$  is a sum of weighted Lorentzians

$$F(\omega - \omega_{mm\pm 1}^{\sigma\sigma'}) = \frac{1}{2\pi} \left[ \frac{4D_R}{(\omega - \omega_{mm\pm 1}^{\sigma\sigma'})^2 + 16D_R^2} \right] \quad (3.31)$$

centered around the allowed frequency transfers  $\omega = \omega_{mm\pm 1}^{\sigma\sigma'}$  and of width  $8D_R$  (full width half maximum). Since  $D_R$  has dimension  $\text{s}^{-1}$ , it follows from Eq. (3.22) that  $\zeta$  has the dimension of an action. We write  $\zeta = \zeta_n h$ , where  $\zeta_n$  is a dimensionless number taken as parameter. We then obtain  $D_R = 2.08 \times 10^{10}(T/\zeta_n) \text{ s}^{-1}$  where  $T$  is measured in Kelvin. Equivalently,  $D_R = 0.694(T/\zeta_n) \text{ cm}^{-1}$ . Since to our knowledge there are so far no direct measurements of the orientational dynamics of the  $\text{C}_{84}$  molecule in  $\text{Sc}_2\text{C}_2@\text{C}_{84}$ , we will choose a value of  $D_R$  such that the correlation time  $\tau_c = (4D_R)^{-1}$  has a value that is intermediate between the values of 2 ns and 5 ps measured by NMR experiments for the  $\text{C}_{70}$  molecule in the low-temperature monoclinic and high-temperature fcc phases of solid  $\text{C}_{70}$ , respectively [16]. Assuming that  $\zeta_n = 100$  is a realistic value (then  $D_R = 10^{10} \text{ s}^{-1}$  at  $T = 50 \text{ K}$ ), we have plotted the scattering function  $C(\omega)$  for several temperatures in Fig. 5. The resonances are centered at the frequency transfers  $\omega_{mn}^{\sigma\sigma'}$  for the potential strength  $q = 2$ . The spectra reflect the characteristic assymmetries for  $\omega > 0$  and  $\omega < 0$  due to anti-Stokes and Stokes processes, respectively. In our calculations, we have included transitions with the values  $m, n = 0, \dots, 19$ .

We notice that if one artificially excludes the tunneling motion of the  $\text{C}_2$  unit by taking a fixed value, say 0, for the angle  $\tau$ , one finds that  $Q^{ss}(\omega) = 0$  and  $Q^{cc} = \delta(\omega)$ . Then Eq. (3.25) becomes  $C(\omega) = F(\omega)$ . Since the  $\text{C}_2$ -unit is dragged along with the classical rotational diffusion of the encapsulating  $\text{C}_{84}$  molecule, its polarizability is changing accordingly with time and the Raman scattering laws  $R_{ZZZZ}(\omega)$  and  $R_{ZYZY}(\omega)$  will exhibit a Lorentzian  $F(\omega)$  of width  $4D_R$  centered at  $\omega = 0$ .

#### IV. POWDER AVERAGES

In Sect. III we have considered a cubic crystal with crystal axes  $(X', Y', Z')$  in coincidence with the laboratory-fixed cubic axes  $(X, Y, Z)$ . Since experiments are performed on powder samples, we will extend the previous results. The powder sample consists of a large number of arbitrarily oriented cubic crystallites, each crystallite has symmetry  $Fm\bar{3}m$  where the  $\text{Sc}_2\text{C}_2@\text{C}_{84}$  units are meroaxially disordered [4]. We first will consider one single crystallite

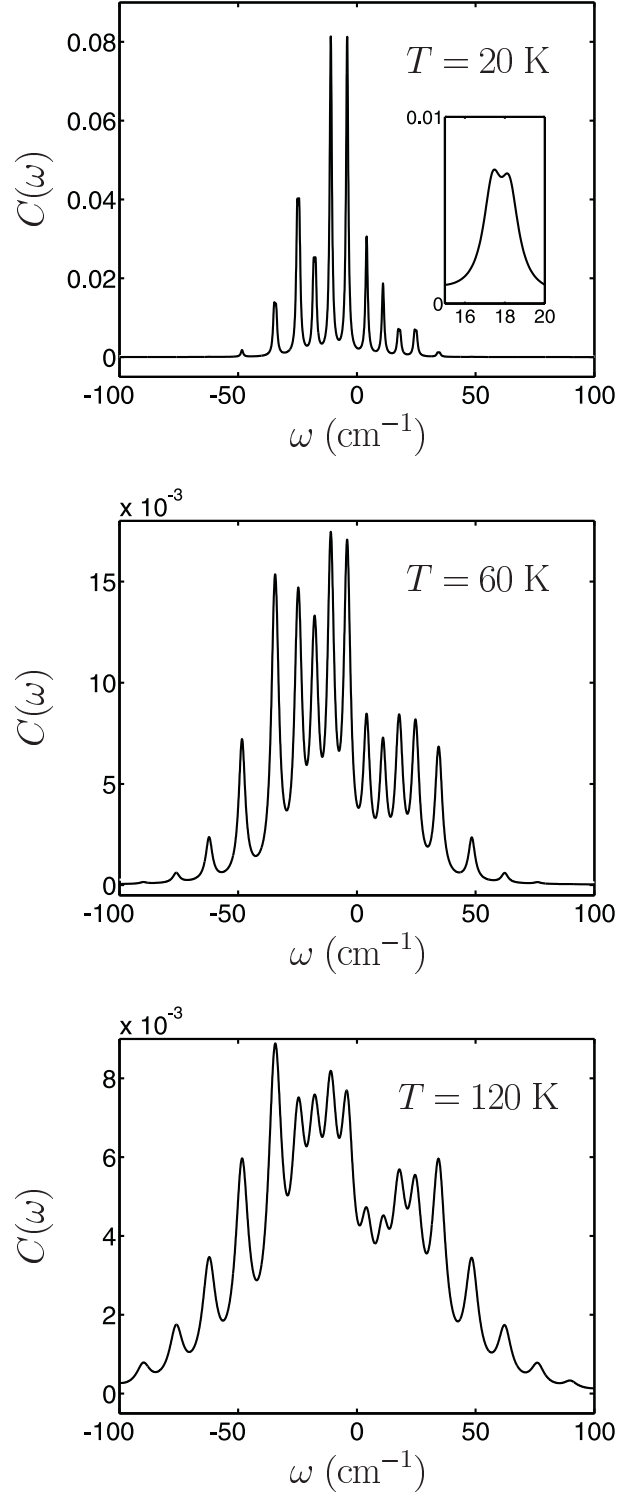


FIG. 5: Scattering function  $C(\omega)$  for  $T = 20 \text{ K}$ ,  $60 \text{ K}$  and  $120 \text{ K}$ . The width  $8D_R$  is the same for all resonance lines and increases linearly from  $1.11 \text{ cm}^{-1}$  to  $6.66 \text{ cm}^{-1}$  for  $T = 20 \text{ K}$  and  $120 \text{ K}$ , respectively. The inset at  $T = 20 \text{ K}$  shows the splitting of the  $\omega_{12}^{--}$  and  $\omega_{12}^{+-}$  resonances.

where the crystal-fixed system of axes is related to the laboratory-fixed system of axes by the Euler angles  $(\alpha, \beta, \gamma)$ . The  $C_2$  rotors are now moving in planes normal to the  $X'$ ,  $Y'$ ,  $Z'$  axes of the rotated coordinate system. This means that the polarizabilities  $\alpha_{ZZ}^R$  or  $\alpha_{ZY}^R$  measured in the laboratory-fixed coordinate system will depend on the Euler angles of the given crystallite.

In Appendix B we have calculated the polarizability components  $\alpha_{ZZ}^{(i)R}$  which are obtained from  $\alpha_{ZZ}^{(i)}$  by application of the rotation operation  $R(\alpha, \beta, \gamma)$ :

$$\alpha_{ZZ}^{(i)R} = R(\alpha, \beta, \gamma) \alpha_{ZZ}^{(i)}. \quad (4.1)$$

The meroaxial average

$$\alpha_{ZZ}^R = \frac{1}{3} \sum_{i=1}^3 \alpha_{ZZ}^{(i)R} \quad (4.2)$$

is obtained as

$$\alpha_{ZZ}^R = a + \frac{b}{3} \sum_{i=1}^3 [A_{ZZ}^{(i)}(\beta, \gamma) + B_{ZZ}^{(i)}(\beta, \gamma) \sin 2\theta + C_{ZZ}^{(i)}(\beta, \gamma) \cos 2\theta]. \quad (4.3)$$

where  $i = 1$  refers to  $\xi \parallel X'$ ,  $i = 2$  to  $\xi \parallel Y'$  and  $i = 3$  to  $\xi \parallel Z'$ . The coefficients  $A_{ZZ}^{(i)}(\beta, \gamma)$ ,  $B_{ZZ}^{(i)}(\beta, \gamma)$  and  $C_{ZZ}^{(i)}(\beta, \gamma)$  are derived in Appendix B, they are found to depend on only two Euler angles.

In the present section we assume that the meroaxial disorder is static or equivalently there are no reorientations of the  $C_{84}$  molecules among the three meroaxial directions in a given crystallite. The angle  $\theta$  is then the sole dynamic quantity. The time-dependent polarizability correlation function per molecule in the given crystallite is obtained as

$$\langle \alpha_{ZZ}^R(t) \alpha_{ZZ}^R(0) \rangle = a^2 + \frac{b^2}{9} \sum_{i,j} [A_{ZZ}^{(i)} A_{ZZ}^{(j)} + B_{ZZ}^{(i)} B_{ZZ}^{(j)} S(t) + C_{ZZ}^{(i)} C_{ZZ}^{(j)} C(t)]. \quad (4.4)$$

The correlation functions  $C(t)$  and  $S(t)$ , defined by Eqs. (2.12) and (2.13) respectively, have been calculated in Sects. II and III.

The powder average for a function  $F(\beta, \gamma)$  is defined as

$$\bar{F} = \frac{1}{4\pi} \int_0^{2\pi} d\gamma \int_0^\pi d\beta \sin \beta F(\beta, \gamma). \quad (4.5)$$

The results for the products  $\overline{A_{ZZ}^{(i)} A_{ZZ}^{(j)}}$ ,  $\overline{B_{ZZ}^{(i)} B_{ZZ}^{(j)}}$ , ... are quoted in Appendix B. The powder-averaged polarizability correlation function per molecule reads

$$\overline{\langle \alpha_{ZZ}^R(t) \alpha_{ZZ}^R(0) \rangle} = a^2 + \frac{b^2}{9} \left[ \frac{8}{15} S(t) + \frac{12}{15} C(t) \right]. \quad (4.6)$$

Taking into account  $S(t) = C(t)$ , Eq. (3.23), we obtain the Raman scattering law for a powder-averaged sample with meroaxial disorder:

$$\overline{R_{ZZZZ}(\omega)} = N \left( a^2 \delta(\omega) + \frac{4}{27} b^2 C(\omega) \right). \quad (4.7)$$

The expression for a single crystal with meroaxial disorder has been given by Eq. (2.26).

In an analogous way one calculates

$$\alpha_{ZY}^R = \frac{1}{3} \sum_{i=1}^3 \alpha_{ZY}^{(i)R} \quad (4.8)$$

with the result

$$\alpha_{ZY}^R = \frac{b}{3} \sum_{i=1}^3 [A_{ZY}^{(i)}(\alpha, \beta, \gamma) + B_{ZY}^{(i)}(\alpha, \beta, \gamma) \sin 2\theta + C_{ZY}^{(i)}(\alpha, \beta, \gamma) \cos 2\theta]. \quad (4.9)$$

The coefficients  $A_{ZY}^{(i)}, \dots, C_{ZY}^{(i)}$  are given in Appendix B. The time-dependent polarizability correlation function per molecule reads

$$\langle \alpha_{ZY}^R(t) \alpha_{ZY}^R(0) \rangle = \frac{b^2}{9} \sum_{i,j} [A_{ZY}^{(i)} A_{ZY}^{(j)} + B_{ZY}^{(i)} B_{ZY}^{(j)} S(t) + C_{ZY}^{(i)} C_{ZY}^{(j)} C(t)]. \quad (4.10)$$

The powder average of a function  $F(\alpha, \beta, \gamma)$  is defined by

$$\overline{F} = \frac{1}{8\pi^2} \int_0^{2\pi} d\alpha \int_0^{2\pi} d\gamma \int_0^\pi d\beta \sin \beta F(\alpha, \beta, \gamma). \quad (4.11)$$

Taking into account the powder averages  $\overline{A_{ZY}^{(i)} A_{ZY}^{(j)}}$  etc., calculated in Appendix B, we obtain

$$\overline{\langle \alpha_{ZY}^R(t) \alpha_{ZY}^R(0) \rangle} = \frac{b^2}{9} \left[ \frac{11}{15} S(t) + \frac{4}{15} C(t) \right]. \quad (4.12)$$

The Raman scattering law then reads

$$\overline{R_{ZYZY}(\omega)} = N \frac{b^2}{9} C(\omega), \quad (4.13)$$

where again we have used  $S(t) = C(t)$ , Eq. (3.23). We see that the powder-averaged expression is the same as the one for a single crystal with meroaxial disorder, Eq. (2.28).

## V. DYNAMIC MEROAXIAL DISORDER

So far we have assumed that the orientation of the long axis ( $S_4$ ) of the  $C_{84}$  molecule in a given cubic crystallite along the equivalent  $\langle 100 \rangle$  directions is random but static. The sole effect of the heat bath was the uniaxial rotational diffusion studied in Sect. III B. While this situation of static meroaxial disorder is realistic at temperatures inferior to say 100 K, it becomes less valid at higher  $T$ . Here again we refer to the situation in solid  $C_{70}$  where with increasing temperature it is found that the uniaxial rotation axis flips between different symmetry equivalent orientations such that the rotational motion becomes more and more isotropic [12, 13, 14, 15, 16, 17]. We therefore will extend the previous model and take into account the situation where a molecule at a given lattice site in one crystallite changes orientation with the  $S_4$  axis jumping randomly between equivalent potential minima in  $\langle 100 \rangle$  directions. Here the heat bath causes stochastic torques about axes perpendicular to the long axis of the  $C_{84}$  molecule or equivalently perpendicular to the rotation axis of the encapsulated  $Sc_2C_2$  quantum gyroscope. We recall that accordingly the normal to the plane of the  $C_2$  quantum rotor will change its orientation. Within a simple three sites stochastic jump model (see e.g. [20]), the conditional probability  $p(i, t|j, 0)$  to find a  $C_{84}$  molecule in an orientation  $i = 1, 2, 3$  at time  $t \geq 0$  when it was in orientation  $j = 1, 2, 3$  at time 0 is obtained by solving a system of three linear differential equations. One obtains

$$p(i, t|j, 0) = \frac{1}{3}(1 + 2e^{-3wt}), \quad i = j, \quad (5.1)$$

$$p(i, t|j, 0) = \frac{1}{3}(1 - e^{-3wt}), \quad i \neq j, \quad (5.2)$$

where  $w$  is the transition rate for a molecular reorientation. We associate the transition rate with the inverse of a relaxation time:

$$w = \frac{1}{\tau} = \frac{1}{\tau_0} e^{-E_a/T}. \quad (5.3)$$

Here we have assumed an Arrhenius-type law, known from reaction rate theory [26, 29], where  $1/\tau_0$  is an attempt frequency and  $E_a$  an activation energy for meroaxial reorientations of the  $Sc_2C_2@C_{84}$  complex as a whole. The equilibrium value of the conditional probability is independent of the initial and final orientation and corresponds to an a priori probability:

$$\lim_{t \rightarrow \infty} p(i, t|j, 0) = \frac{1}{3}. \quad (5.4)$$

In the previous section the meroaxial orientations within a given crystallite have been characterized by the coefficients  $\{A_{ZZ}^{(i)}, B_{ZZ}^{(i)}, C_{ZZ}^{(i)}\}$ ,  $\{A_{ZY}^{(i)}, B_{ZY}^{(i)}, C_{ZY}^{(i)}\}$  in Eqs. (4.3) and (4.9) of the polarizabilities  $\alpha_{ZZ}^R$  and  $\alpha_{ZY}^R$ . Treating these coefficients as dynamic stochastic quantities we obtain instead of Eqs. (4.4) and (4.10)

$$\begin{aligned}\langle \alpha_{ZZ}^R(t)\alpha_{ZZ}^R(0) \rangle &= a^2 + b^2 \left[ \langle A_{ZZ}(t)A_{ZZ}(0) \rangle \right. \\ &\quad \left. + \langle B_{ZZ}(t)B_{ZZ}(0) \rangle S(t) + \langle C_{ZZ}(t)C_{ZZ}(0) \rangle C(t) \right],\end{aligned}\quad (5.5)$$

$$\begin{aligned}\langle \alpha_{ZY}^R(t)\alpha_{ZY}^R(0) \rangle &= b^2 \left[ \langle A_{ZY}(t)A_{ZY}(0) \rangle \right. \\ &\quad \left. + \langle B_{ZY}(t)B_{ZY}(0) \rangle S(t) + \langle C_{ZY}(t)C_{ZY}(0) \rangle C(t) \right].\end{aligned}\quad (5.6)$$

The correlation functions  $\langle A_{ZZ}(t)A_{ZZ}(0) \rangle, \dots, \langle C_{ZY}(t)C_{ZY}(0) \rangle$  which refer to meroaxial reorientations are calculated within the frame of the stochastic jump model. For instance for a given set  $\{A^{(i)}, i = 1, 2, 3\}$  one has

$$\langle A(t)A(0) \rangle = \frac{1}{3} \sum_{i,j} A^{(i)} A^{(j)} p(i, t|j, 0), \quad (5.7)$$

where the conditional probabilities  $p(i, t|j, 0)$  are given by Eqs. (5.1) and (5.2), while the factor 1/3 accounts for the equilibrium initial probability. Since the coefficients  $A^{(i)}$  depend on the Euler angles which specify the orientation of a given crystallite (Sect. IV), the powder-averaged correlation functions are obtained by averaging over the Euler angles:

$$\overline{\langle A(t)A(0) \rangle} = \frac{1}{3} \sum_{i,j} \overline{A^{(i)} A^{(j)}} p(i, t|j, 0). \quad (5.8)$$

Taking into account the values of the powder-averaged products given in Appendix B, we obtain:

$$\overline{\langle A_{ZZ}(t)A_{ZZ}(0) \rangle} = \frac{4}{45} e^{-3t/\tau}, \quad (5.9)$$

$$\overline{\langle B_{ZZ}(t)B_{ZZ}(0) \rangle} = \frac{8}{135} [1 + 2e^{-3t/\tau}], \quad (5.10)$$

$$\overline{\langle C_{ZZ}(t)C_{ZZ}(0) \rangle} = \frac{12}{135} [1 + 3e^{-3t/\tau}]. \quad (5.11)$$

The powder average of Eq. (5.5) then reads

$$\overline{\langle \alpha_{ZZ}^R(t)\alpha_{ZZ}^R(0) \rangle} = a^2 + \frac{4b^2}{27} D(t), \quad (5.12)$$

where the function  $D(t)$  is given by

$$D(t) = \left[ C(t) + \frac{3}{5}e^{-3t/\tau} + \frac{13}{5}C(t)e^{-3t/\tau} \right]. \quad (5.13)$$

Here we have used again  $C(t) = S(t)$ , Eq. (3.23). The first term on the right-hand side  $C(t)$  accounts for the superposition of the quantum motion (tunneling) of the  $C_2$  rotor and the uniaxial rotational diffusion of the encapsulating  $C_{84}$  molecule, the second term  $\propto e^{-3t/\tau}$  accounts for the classical motion of the  $C_2$  rotor when its plane of motion is changing with the meroaxial reorientations of the encapsulating  $C_{84}$  molecule, finally the third term  $\propto C(t)e^{-3t/\tau}$  accounts for the interference of the two motions of the  $C_{84}$  molecule with the tunneling of the  $C_2$  rotor.

Similarly, using again Eq. (5.8) and the powder-averaged products  $\overline{(A_{ZY}^{(i)})^2}$  etc. in Appendix B, we find

$$\overline{\langle A_{ZY}(t)A_{ZY}(0) \rangle} = \frac{1}{15}e^{-3t/\tau}, \quad (5.14)$$

$$\overline{\langle B_{ZY}(t)B_{ZY}(0) \rangle} = \frac{11}{135} [1 + 2e^{-3t/\tau}], \quad (5.15)$$

$$\overline{\langle C_{ZY}(t)C_{ZY}(0) \rangle} = \frac{1}{135} [4 + 17e^{-3t/\tau}], \quad (5.16)$$

and hence

$$\overline{\langle \alpha_{ZY}^R(t)\alpha_{ZY}^R(0) \rangle} = \frac{b^2}{9}D(t), \quad (5.17)$$

with  $D(t)$  again given by Eq. (5.13). In the limit of small relaxation time we recover Eq. (4.12) for static meroaxial disorder. The Raman scattering laws are given by

$$\overline{R_{ZZZZ}(\omega)} = N \left( a^2 \delta(\omega) + \frac{4}{27}b^2 D(\omega) \right), \quad (5.18)$$

and

$$\overline{R_{ZYZY}(\omega)} = N \frac{b^2}{9} D(\omega). \quad (5.19)$$

The Fourier transform of  $D(t)$  leads to the scattering function

$$D(\omega) = C(\omega) + \frac{3}{5}J(\omega) + \frac{13}{5}G(\omega). \quad (5.20)$$

The spectral function  $C(\omega)$  is given by Eqs. (3.26) – (3.31) while

$$J(\omega) = \frac{1}{\pi} \frac{(3/\tau)}{\omega^2 + (3/\tau)^2}, \quad (5.21)$$

is the Fourier transform of the relaxation function  $e^{-3t/\tau}$ . The Fourier transform of the interference term

$$G(\omega) = \frac{1}{2\pi} \int_{-\infty}^{+\infty} dt e^{-i\omega t} C(t) e^{-3|t|/\tau} \quad (5.22)$$

is rewritten as

$$G(\omega) = \int_{-\infty}^{+\infty} d\omega' C(\omega - \omega') J(\omega'). \quad (5.23)$$

Using Eqs. (3.26) – (3.31) and (5.21) we obtain the scattering function

$$G(\omega) = G_{++}(\omega) + G_{--}(\omega) + G_{+-}(\omega) + G_{-+}(\omega). \quad (5.24)$$

The functions  $G_{++}(\omega), \dots, G_{--}(\omega)$  have the same structure as  $C_{++}(\omega), \dots, C_{--}(\omega)$ , Eqs. (3.27) – (3.30), respectively, but where the Lorentzians  $F(\omega - \omega_{mm\pm 1}^{\sigma\sigma'})$ , Eq. (3.31), are replaced by

$$H(\omega - \omega_{mm\pm 1}^{\sigma\sigma'}) = \frac{1}{2\pi} \left[ \frac{\Gamma}{(\omega - \omega_{mm\pm 1}^{\sigma\sigma'})^2 + \Gamma^2} \right]. \quad (5.25)$$

Similarly to  $C(\omega)$ , Eq. (3.26), the function  $G(\omega)$  is a sum of weighted Lorentzians centered around  $\omega = \omega_{mm\pm 1}^{\sigma\sigma'}$  but of width  $2\Gamma$  where

$$\Gamma = 4D_R + 3/\tau. \quad (5.26)$$

The broadening of the transition frequencies of the quantum rotor with increasing temperature is now due to the uniaxial rotational diffusion and the meroaxial reorientations of the encapsulating  $C_{84}$  molecule. Notice that both contributions depend on temperature. In Fig. 6 we have plotted the function  $G(\omega)$  for several temperatures. The parameters describing the dynamics of the  $C_{84}$  molecule are  $\zeta_n = 100$  for the rotational diffusion model and  $\tau_0^{-1} = 3 \times 10^{12} \text{ s}^{-1}$  (attempt frequency) and  $E_a = 580 \text{ K}$  (activation energy) for the thermally activated meroaxial reorientations. Comparable values of the activation energy, i.e. 32(7) meV and 35(15) meV have been deduced from neutron scattering studies in solid  $C_{70}$  [17] and solid  $C_{60}$  [27], respectively. While for  $T = 20 \text{ K}$  and  $60 \text{ K}$  the contribution of  $3/\tau$  to the half width  $\Gamma$  is negligible in comparison to  $4D_R$ , both (additive) contributions become comparable at 150 K. At higher  $T$  the thermally-activated reorientations are dominant and lead to a smearing out of the low-frequency resonances in the scattering function  $G(\omega)$ .

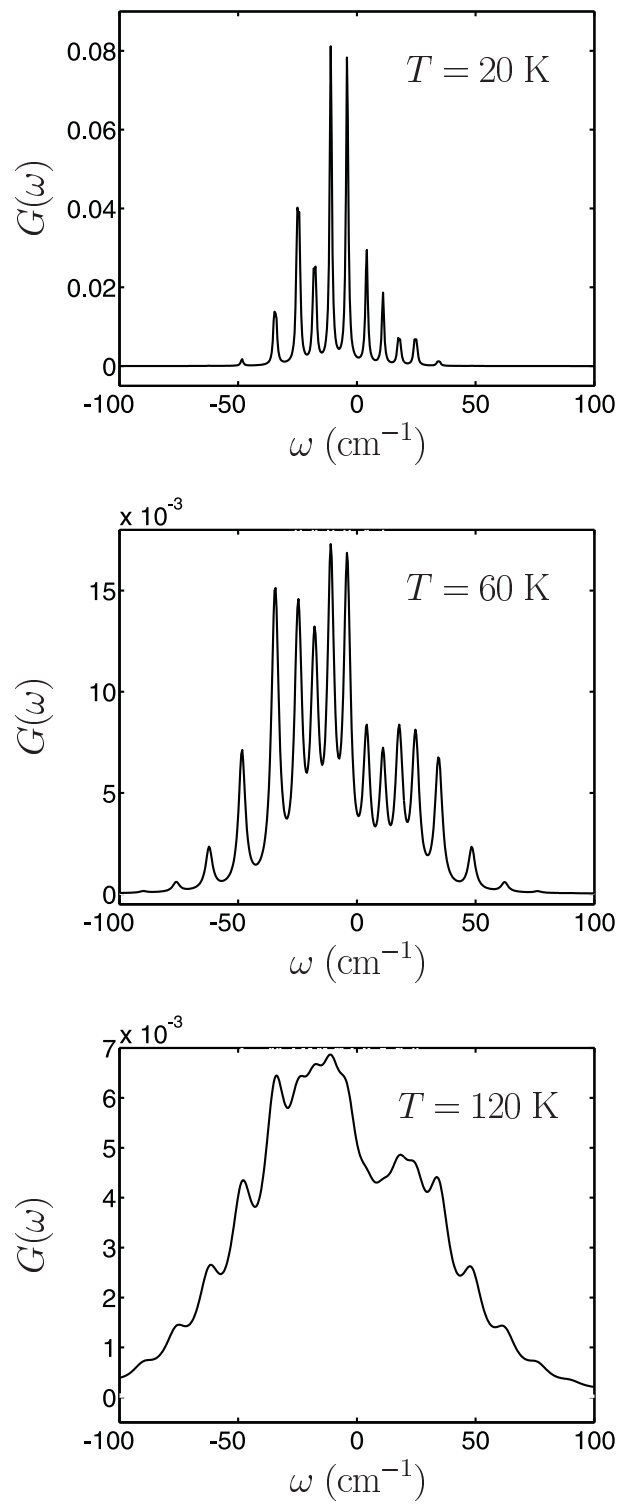


FIG. 6: Scattering function  $G(\omega)$  for  $T = 20 \text{ K}$ ,  $60 \text{ K}$  and  $120 \text{ K}$ .

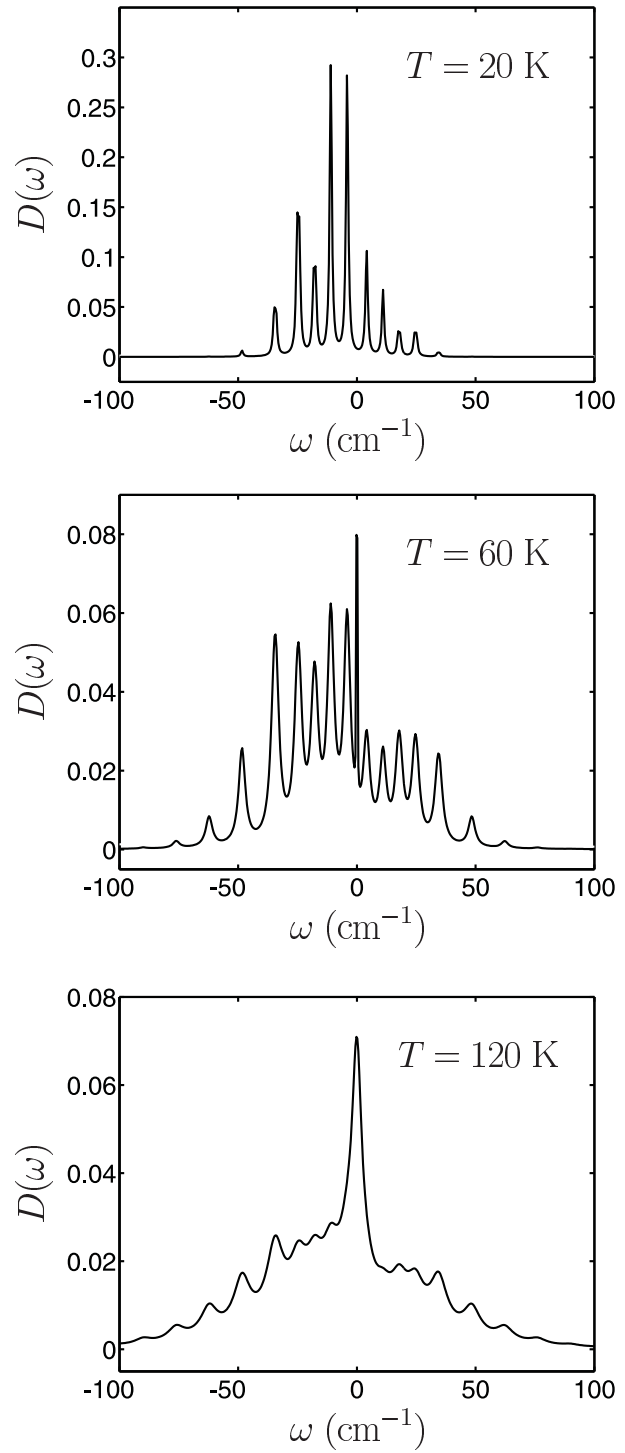


FIG. 7: Spectral function  $D(\omega)$  of the low-frequency Raman scattering laws for  $T = 20 \text{ K}$ ,  $60 \text{ K}$ ,  $120 \text{ K}$ .

If one would artificially exclude the tunneling motion, the function  $D(\omega)$  entering the Raman scattering laws of the  $C_2$  unit would reduce to a superposition of Lorentzians centered at  $\omega = 0$ :

$$D(\omega) = F(\omega) + \frac{3}{5}J(\omega) + \frac{13}{5}H(\omega). \quad (5.27)$$

The first term on the right-hand side [given by Eq. (3.24)] accounts solely for the rotational uniaxial diffusion, the second term for the meroaxial reorientations and the last term for the interference of these classical motions of the encapsulating  $C_{84}$  molecule.

## VI. DISCUSSION

It has been shown that the low-frequency (rotational) part of the Raman scattering spectrum of a powder crystal of  $Sc_2C_2@C_{84}$  fullerite reflects the superposition of the quantum tunneling motion of the encapsulated  $Sc_2C_2$  complex about its long axis and the random classical rotational motion of the surrounding  $C_{84}$  molecule. The effect of the  $C_{84}$  molecule on the dynamics of  $Sc_2C_2$  is twofold. Firstly, since the long axis of  $Sc_2C_2$  gyroscope coincides with the  $S_4$  axis of the molecule, the rotation of  $Sc_2C_2$  about this axis corresponds to the motion of the  $C_2$  bond as a planar quantum rotor in a fourfold potential [6]. Secondly, any rotation of the  $C_{84}$  molecule caused by torques due to the thermal lattice environment leads to a dragging of the enclosed  $Sc_2C_2$  unit and hence affects the spectrum of the  $C_2$  quantum rotor seen in the laboratory frame. The low-frequency Raman spectra resulting from the interaction of the scattering radiation with the induced dipole of the  $C_2$  rotor reflect these features.

In analogy with the dynamics of the  $C_{70}$  molecule in solid  $C_{70}$  [17], we have assumed that the rotational motion of the  $C_{84}$  molecule at a lattice site in a given crystallite is composed of two parts: uniaxial rotational diffusion about the  $S_4$  axis and stochastic jumps of the  $S_4$  orientation among  $\langle 100 \rangle$  directions. The superposition of the tunneling motion of the planar quantum rotor with the classical rotations of the  $C_{84}$  molecule leads to the spectral function

$$D(\omega) = C(\omega) + \frac{3}{5}J(\omega) + \frac{13}{5}G(\omega), \quad (6.1)$$

given by Eq. (5.20), in the Raman scattering laws  $R_{ZZZZ}(\omega)$  and  $R_{ZYZY}(\omega)$ .

The function  $C(\omega)$ , defined by Eqs. (3.25) – (3.31), accounts for tunneling transitions between the energy levels of the encapsulated  $C_2$  rotor. The spectrum consists of a series of

resonances described by Lorentzians centered at the transition frequencies (Table I,  $q = 2$ ) and broadened by the uniaxial rotational diffusion (half width  $4D_R$ ) of the surrounding  $C_{84}$  molecule. Since the hindering potential for the rotational diffusion about the  $S_4$  axis is weak, this motion affects the spectrum already at low  $T$ . The temperature dependence of the spectrum has been studied in Fig. 5.

The term  $J(\omega)$  in Eq. (6.1) accounts for the Raman spectrum of the radiation-induced  $C_2$  dipole while the  $Sc_2C_2$  unit is dragged along by the classical reorientations of the  $C_{84}$  molecule among its three meroaxial directions. This motion which reflects the changes of the orientation of the  $C_2$  rotor plane is described by a three sites stochastic jump model, characterized by a thermally activated relaxation time  $\tau = \tau_0 e^{E_a/T}$ . Notice that  $J(\omega)$  leads to a central resonance of half width  $(3/\tau)$  in the Raman scattering law even in absence of any quantum mechanical tunneling of  $C_2$ . The width of this central resonance (quasi-elastic peak) becomes appreciable at  $T \geq 100$  K. In the scattering law  $\overline{R_{ZZZZ}}(\omega)$ , Eq. (5.18), this quasi-elastic peak is present in addition to the elastic Rayleigh peak. We suggest that in future low-energy Raman experiments additional attention will be given to the possible identification of the temperature-dependent quasi-elastic peak.

The last term  $G(\omega)$  in Eq. (6.1) is due to the interference between the uniaxial diffusion-modulated tunneling motion described by  $C(\omega)$  and the stochastic jump model accounted for by  $J(\omega)$ . The function  $G(\omega)$  is a convolution of  $C$  and  $J$  [see Eq. (5.23)]. While at low  $T$  the spectra of  $C(\omega)$  and  $G(\omega)$  are very similar (compare the plots for  $T = 20$  K,  $T = 60$  K in Fig. 5 and Fig. 6) they become different at higher  $T$  (see the 120 K plots) where the increasing influence of the stochastic jumps adds to the line broadening. The width  $2\Gamma$  of the individual resonances, Eq. (5.26), increases from  $1.11 \text{ cm}^{-1}$  at  $T = 20$  K to  $3.37 \text{ cm}^{-1}$  at  $T = 60$  K and  $11.43 \text{ cm}^{-1}$  at  $T = 120$  K. This broadening leads to an overlap of the low-frequency resonances with increasing  $T$ .

Finally the sum  $D(\omega)$  of these contributions which corresponds to the low-frequency Raman response function is shown in Fig. 7. The quasi-elastic peak centered at  $\omega = 0$  becomes important with increasing temperature. In addition the growing importance of  $G(\omega)$  smears out the low-frequency resonances with increasing  $T$  while the higher frequency resonances remain prominent.

The overall shape of the spectral function  $D(\omega)$  and its temperature evolution agree very well with the low-frequency Raman scattering results of Ref. 6. There is quantitative

agreement with the position of the resonance lines. The smearing out of the low-frequency resonances and the prominence of the higher-frequency resonances with increasing  $T$  (Fig. 3 of Ref. 6) are well reproduced by the present theory. In addition to the positions of the resonance lines, the theory accounts for their temperature-dependent broadening. In Fig. 8 we confront the theoretical spectra  $D(\omega)$  with the experimental Raman spectra, for both  $T = 60$  K and  $T = 120$  K. We notice that the experimental spectra are contaminated by a plasma line at  $-\omega = 29.6$  cm<sup>-1</sup> [6]. Note that the central parts of the experimental spectra have been omitted in order to remove the effect of the unshifted Rayleigh peak. On the other hand the theoretical spectrum exhibits a quasi-elastic peak which is an intrinsic effect due to the meroaxial stochastic reorientations of the Sc<sub>2</sub>C<sub>2</sub>@C<sub>84</sub> complex [contribution  $J(\omega)$  in  $D(\omega)$ ]. Complementary to the present work it would be useful to measure the dynamics of the C<sub>84</sub> molecule in solid Sc<sub>2</sub>C<sub>2</sub>C<sub>84</sub> directly say by NMR, neutron or  $\mu$ -spin spectroscopy.

### Acknowledgments

The theoretical work has been supported by the Bijzonder Onderzoeksfonds, Universiteit Antwerpen (BOF-UA). B.V. is a Postdoctoral Fellow of the Research Foundation - Flanders (FWO). The experimental work has been supported by the EU Project NANOTEMP and by the Austrian FWF (17345-PHY).

### APPENDIX A

We recall that  $\nu$  is the angle of rotation of the C<sub>84</sub> molecule about its  $S_4$  axis. Treating the molecule as a Brownian rotor we have the one-dimensional Langevin equation

$$\Theta\ddot{\nu}(t) + \zeta\dot{\nu}(t) = \lambda(t) - \frac{\partial U}{\partial\nu}. \quad (\text{A1})$$

Here  $\Theta$  is the moment of inertia about the  $S_4$  axis,  $\zeta\dot{\nu}$  is the friction torque,  $\lambda(t)$  a white noise driving torque and  $-\partial U/\partial\nu$  is a torque due to the orientational crystal field potential  $U(\nu(t))$ . Under the assumption [26] that the friction torque is dominant in comparison to the inertial term and that the variation of  $U$  with  $\nu$  is weak, one can use standard methods [11] to derive a Smoluchowski equation for the angular distribution function  $w(\nu(t))$ :

$$\frac{\partial w}{\partial t} = D_R \frac{\partial^2 w}{\partial \nu^2}, \quad (\text{A2})$$

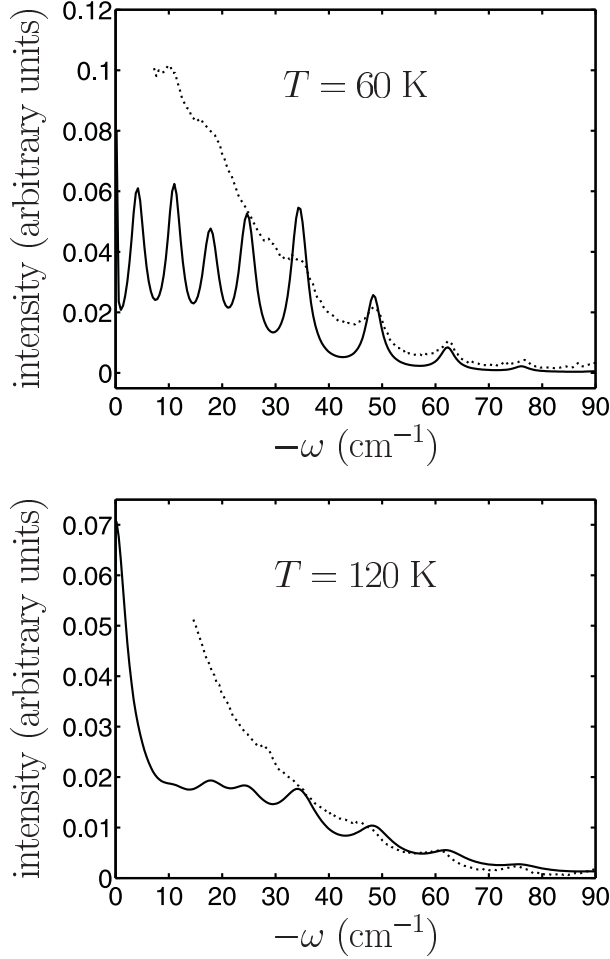


FIG. 8: Comparison of theoretical scattering law  $D(\omega)$  (solid line), calculated at  $T = 60$  K and  $T = 120$  K, with experimental Raman results (dotted line) taken at the respective temperatures.

where  $D_R = k_B T / \zeta$ .

The functions

$$\{\psi_m(\nu)\} = \left\{ \frac{e^{im\nu}}{\sqrt{2\pi}} \right\}, \quad (\text{A3})$$

$m = 0, \pm 1, \dots$  are orthonormal eigenfunctions of the operator  $\partial^2 / \partial \nu^2$  with eigenvalues  $\{0, -1, -m^2, \dots\}$ . We calculate the conditional probability distribution  $w(\nu, t | \nu_0, 0)$  to find the molecule at an angle  $\nu$  at time  $t$  when it was at angle  $\nu_0$  at  $t = 0$ . The initial condition can be written as

$$\lim_{t \rightarrow 0} w(\nu, t | \nu_0, 0) = \delta(\nu - \nu_0) = \sum_m \psi_m^*(\nu) \psi_m(\nu_0), \quad (\text{A4})$$

where the second member equality is just the closure relation. On the other hand in the long-time limit the orientation of the molecule should be random which corresponds to the

condition

$$\lim_{t \rightarrow \infty} w(\nu, t | \nu_0, 0) = \frac{1}{2\pi}. \quad (\text{A5})$$

A particular solution of (A2) subject to these boundary condition is of the form

$$w(\nu, t | \nu_0, 0) = \sum_m e^{-D_R m^2 t} \psi_m^*(\nu) \psi_m(\nu_0). \quad (\text{A6})$$

The correlation function  $\langle \cos 2\nu(t) \cos 2\nu(0) \rangle$ , Eq. (2.20), is rewritten as a thermal average:

$$F^{cc}(t) = \int_0^{2\pi} d\nu \int_0^{2\pi} d\nu_0 \cos 2\nu G(\nu, t | \nu_0, 0) \cos 2\nu_0. \quad (\text{A7})$$

Here  $G(\nu, t | \nu_0, 0) d\nu d\nu_0$  is the joint probability of finding the  $C_{84}$  molecule with orientation angle  $\nu_0 \equiv \nu(0)$  in the interval  $d\nu_0$  initially and orientation  $\nu \equiv \nu(t)$  in  $d\nu$  at time  $t$ . One has

$$G(\nu, t | \nu_0, 0) = w(\nu, t | \nu_0, 0) p(\nu_0), \quad (\text{A8})$$

where the conditional probability  $w(\nu, t | \nu_0, 0)$  is given by

$$w(\nu, t | \nu_0, 0) = \frac{1}{2\pi} \sum_m e^{-m^2 D_R t} e^{im(\nu - \nu_0)}, \quad (\text{A9})$$

$m = 0, \pm 1, \dots$ , and where  $p(\nu_0) = 1/2\pi$  is the initial equilibrium probability. Carrying out the integrals in Eq. (A7) gives as a result Eq. (3.20). In a similar way we obtain Eq. (3.21).

## APPENDIX B

Here we give details about the calculation of the powder averages in Sect. IV. We start from the situation where the  $C_{84}$  molecule is in standard orientation, which corresponds to the polarizabilities  $\alpha_{ZZ}^{(1)}$  and  $\alpha_{ZY}^{(1)}$  given by Eqs. (2.3) and (2.9) respectively. In order to apply the rotation operation  $R(\alpha, \beta, \gamma)$  we rewrite the polarizabilities in terms of spherical harmonics  $Y_l^m(\theta, \phi)$ . We use the notations and conventions of Bradley and Cracknell [28].

With

$$Y_2^0(\theta) = \left( \frac{5}{16\pi} \right)^{1/2} (3 \cos^2 \theta - 1), \quad (\text{B1})$$

$$Y_2^{\pm 1}(\theta, \phi) = \left( \frac{15}{8\pi} \right)^{1/2} \cos \theta \sin \theta e^{\pm i\phi}, \quad (\text{B2})$$

we get

$$\alpha_{ZZ}^{(1)} = a + b \left( \frac{64\pi}{45} \right)^{1/2} Y_2^0(\theta) \Big|_{\phi=\pi/2}, \quad (B3)$$

$$\alpha_{ZY}^{(1)} = -ib \left( \frac{8\pi}{15} \right)^{1/2} [Y_2^1(\theta, \phi) - Y_2^{-1}(\theta, \phi)] \Big|_{\phi=\pi/2}. \quad (B4)$$

The condition  $\phi = \pi/2$  ensures that the  $C_2$  rotor initially moves in the  $(Y, Z)$  plane. Although the function  $Y_2^0(\theta)$  does not depend on  $\phi$ , the condition  $\phi = \pi/2$  has to be taken into account after the application of a rotation operation. The transformation law of spherical harmonics under a rotation  $R(\alpha, \beta, \gamma)$  reads:

$$R(\alpha, \beta, \gamma) Y_l^m(\theta, \phi) = \sum_{n=-l}^{+l} Y_l^n(\theta, \phi) \mathcal{D}_{nm}^l(\alpha, \beta, \gamma). \quad (B5)$$

Here  $\mathcal{D}_{nm}^l(\alpha, \beta, \gamma)$  are the Wigner rotator functions defined by

$$\mathcal{D}_{nm}^l(\alpha, \beta, \gamma) = C_{nm} e^{-in\gamma} d_{nm}^l(\beta) e^{-im\alpha}, \quad (B6)$$

where  $C_{nm} = i^{|n|+n} i^{-|m|-m}$  [28]. The functions  $d_{nm}^l(\beta)$  are polynomials in  $\sin(\beta/2)$  and  $\cos(\beta/2)$ . They satisfy the relations

$$d_{nm}^l(\beta) = (-1)^{n+m} d_{-n, -m}^l(\beta) = (-1)^{n+m} d_{mn}^l(\beta). \quad (B7)$$

We recall that the angles  $\theta$  and  $\phi$  on the right-hand side of Eq. (B5) refer to the values before the application of the rotation. Applying  $R(\alpha, \beta, \gamma)$  to  $\alpha_{ZZ}^{(1)}$ , Eq. (B3), we have to evaluate

$$R(\alpha, \beta, \gamma) Y_2^0(\theta) \Big|_{\phi=\pi/2} = \sum_{n=-2}^{+2} Y_2^n(\theta, \pi/2) \mathcal{D}_{n0}^2(\alpha, \beta, \gamma). \quad (B8)$$

In addition to the definitions (B1) and (B2) we quote

$$Y_2^{\pm 2}(\theta, \pi/2) = -\sqrt{\frac{15}{32\pi}} \sin^2 \theta. \quad (B9)$$

We further use

$$d_{20}^2(\beta) = d_{-20}^2(\beta) = (\sqrt{6}/4) \sin^2 \beta, \quad (B10)$$

$$d_{10}^2(\beta) = d_{-10}^2(\beta) = -(\sqrt{6}/4) \sin 2\beta, \quad (B11)$$

$$d_{00}^2(\beta) = (3 \cos^2 \beta - 1)/2. \quad (B12)$$

We then find after some bookkeeping

$$R(\alpha, \beta, \gamma) Y_2^0(\theta) \Big|_{\phi=\pi/2} = \left( \frac{45}{64\pi} \right)^{1/2} [A_{ZZ}^{(1)}(\beta, \gamma) + B_{ZZ}^{(1)}(\beta, \gamma) \sin 2\theta + C_{ZZ}^{(1)}(\beta, \gamma) \cos 2\theta], \quad (\text{B13})$$

where

$$A_{ZZ}^{(1)}(\beta, \gamma) = \frac{1}{2} \left[ \cos^2 \beta - \sin^2 \beta \cos 2\gamma - \frac{1}{3} \right], \quad (\text{B14})$$

$$B_{ZZ}^{(1)}(\beta, \gamma) = \sin 2\beta \sin \gamma, \quad (\text{B15})$$

$$C_{ZZ}^{(1)}(\beta, \gamma) = \frac{1}{2} [\sin^2 \beta \cos 2\gamma + 3 \cos^2 \beta - 1]. \quad (\text{B16})$$

Hence

$$\alpha_{ZZ}^{(1)R} = a + b [A_{ZZ}^{(1)}(\beta, \gamma) + B_{ZZ}^{(1)}(\beta, \gamma) \sin 2\theta + C_{ZZ}^{(1)}(\beta, \gamma) \cos 2\theta]. \quad (\text{B17})$$

With the change  $(\alpha, \beta, \gamma) \rightarrow (\alpha, \beta, \gamma - \frac{\pi}{2})$  we find the coefficients entering  $\alpha_{ZZ}^{(2)R}$

$$A_{ZZ}^{(2)}(\beta, \gamma) = \frac{1}{2} \left[ \cos^2 \beta + \sin^2 \beta \cos 2\gamma - \frac{1}{3} \right], \quad (\text{B18})$$

$$B_{ZZ}^{(2)}(\beta, \gamma) = -\sin 2\beta \sin \gamma, \quad (\text{B19})$$

$$C_{ZZ}^{(2)}(\beta, \gamma) = \frac{1}{2} [-\sin^2 \beta \cos 2\gamma + 3 \cos^2 \beta - 1], \quad (\text{B20})$$

and with  $(\alpha, \beta, \gamma) \rightarrow (\alpha, \beta + \frac{\pi}{2}, \gamma = 0)$  the coefficients entering  $\alpha_{ZZ}^{(3)R}$

$$A_{ZZ}^{(3)}(\beta, \gamma) = \frac{1}{2} \left[ \sin^2 \beta - \cos^2 \beta - \frac{1}{3} \right], \quad (\text{B21})$$

$$B_{ZZ}^{(3)}(\beta, \gamma) = 0, \quad (\text{B22})$$

$$C_{ZZ}^{(3)}(\beta, \gamma) = \frac{1}{2} [\cos^2 \beta + 3 \sin^2 \beta - 1]. \quad (\text{B23})$$

The average polarizability  $\alpha_{ZZ}^R$  is then given by Eq. (4.3). Applying the definition of powder average Eq. (4.5) we get  $\overline{[A_{ZZ}^{(i)}]^2} = \frac{4}{45}$ ,  $i = 1, 2, 3$ ;  $\overline{[B_{ZZ}^{(i)}]^2} = \frac{4}{15}$ ,  $i = 1, 2$ ;  $\overline{[C_{ZZ}^{(i)}]^2} = \frac{4}{15}$ ,  $i = 1, 2$ ;  $\overline{[C_{ZZ}^{(3)}]^2} = \frac{8}{15}$ ;  $\overline{[A_{ZZ}^{(i)} A_{ZZ}^{(j)}]^2} = -\frac{2}{45}$ ,  $i \neq j$ ;  $\overline{[B_{ZZ}^{(i)} B_{ZZ}^{(j)}]^2} = 0$ ,  $i \neq j$ ;  $\overline{[C_{ZZ}^{(i)} C_{ZZ}^{(j)}]^2} = -\frac{2}{15}$ ,  $i = 1, 2$ ,  $j = 3$ ;  $\overline{[C_{ZZ}^{(1)} C_{ZZ}^{(2)}]^2} = \frac{2}{15}$ .

In a similar way we apply the rotation operation to  $\alpha_{ZY}^{(1)}$ , Eq. (B4), and calculate

$$R(\alpha, \beta, \gamma) Y_2^{\pm 1}(\theta, \pi/2) = \sum_{n=-2}^{+2} Y_2^n(\theta, \pi/2) \mathcal{D}_{n1}^2(\alpha, \beta, \gamma). \quad (\text{B24})$$

Making use of

$$d_{21}^2(\beta) = -\cos^2 \frac{\beta}{2} \sin \beta, \quad d_{11}^2(\beta) = \cos^2 \frac{\beta}{2} (2 \cos \beta - 1), \quad (\text{B25})$$

$$d_{-21}^2(\beta) = \sin^2 \frac{\beta}{2} \sin \beta, \quad d_{-11}^2(\beta) = \sin^2 \frac{\beta}{2} (2 \cos \beta + 1), \quad (\text{B26})$$

$$d_{01}^2(\beta) = \sqrt{6}/4 \sin 2\beta \quad (\text{B27})$$

and of the relations (B7) we find

$$\begin{aligned} & (-i)R(\alpha, \beta, \gamma) [Y_2^1(\theta, \phi) - Y_2^{-1}(\theta, \phi)] \Big|_{\phi=\pi/2} \\ &= \left( \frac{15}{8\pi} \right)^{1/2} [A_{ZY}^{(1)}(\alpha, \beta, \gamma) + B_{ZY}^{(1)}(\alpha, \beta, \gamma) \sin 2\theta + C_{ZY}^{(1)}(\alpha, \beta, \gamma) \cos 2\theta] \end{aligned} \quad (\text{B28})$$

where

$$A_{ZY}^{(1)}(\alpha, \beta, \gamma) = \frac{1}{2} \left[ \sin \beta \sin 2\gamma \cos \alpha + \frac{\sin 2\beta \cos 2\gamma \sin \alpha}{2} + \frac{\sin 2\beta \sin \alpha}{2} \right], \quad (\text{B29})$$

$$B_{ZY}^{(1)}(\alpha, \beta, \gamma) = \cos \beta \cos \gamma \cos \alpha - \cos 2\beta \sin \gamma \sin \alpha, \quad (\text{B30})$$

$$C_{ZY}^{(1)}(\alpha, \beta, \gamma) = \frac{1}{2} \left[ -\sin \beta \sin 2\gamma \cos \alpha - \frac{\sin 2\beta \cos 2\gamma \sin \alpha}{2} + \frac{3 \sin 2\beta \sin \alpha}{2} \right]. \quad (\text{B31})$$

Hence

$$\alpha_{ZY}^{(1)R} = b [A_{ZY}^{(1)}(\alpha, \beta, \gamma) + B_{ZY}^{(1)}(\alpha, \beta, \gamma) + C_{ZY}^{(1)}(\alpha, \beta, \gamma)]. \quad (\text{B32})$$

With the change of angles  $(\alpha, \beta, \gamma - \frac{\pi}{2})$  we get the coefficients entering  $\alpha_{ZY}^{(2)R}$ :

$$A_{ZY}^{(2)}(\alpha, \beta, \gamma) = \frac{1}{2} \left[ -\sin \beta \sin 2\gamma \cos \alpha - \frac{\sin 2\beta \cos 2\gamma \sin \alpha}{2} + \frac{\sin 2\beta \sin \alpha}{2} \right], \quad (\text{B33})$$

$$B_{ZY}^{(2)}(\alpha, \beta, \gamma) = \cos \beta \sin \gamma \cos \alpha + \cos 2\beta \cos \gamma \sin \alpha, \quad (\text{B34})$$

$$C_{ZY}^{(2)}(\alpha, \beta, \gamma) = \frac{1}{2} \left[ -\sin \beta \sin 2\gamma \cos \alpha + \frac{\sin 2\beta \cos 2\gamma \sin \alpha}{2} + \frac{3 \sin 2\beta \sin \alpha}{2} \right], \quad (\text{B35})$$

and with  $(\alpha, \beta, \gamma) \rightarrow (\alpha, \beta + \frac{\pi}{2}, \gamma = 0)$  the coefficients entering  $\alpha_{ZY}^{(3)R}$ :

$$A_{ZY}^{(3)}(\alpha, \beta, \gamma) = -\frac{1}{2} \sin 2\beta \sin \alpha, \quad (\text{B36})$$

$$B_{ZY}^{(3)}(\alpha, \beta, \gamma) = -\sin \beta \cos \alpha, \quad (\text{B37})$$

$$C_{ZY}^{(3)}(\alpha, \beta, \gamma) = -\frac{1}{2} \sin 2\beta \sin \alpha. \quad (\text{B38})$$

With the definition of powder average Eq. (4.11) we get  $\overline{[A_{ZY}^{(i)}]^2} = \frac{1}{15}$ ,  $i = 1, 2, 3$ ;  $\overline{[B_{ZY}^{(i)}]^2} = \frac{1}{5}$ ,  $i = 1, 2$ ;  $\overline{[B_{ZY}^{(3)}]^2} = \frac{1}{3}$ ;  $\overline{[C_{ZY}^{(i)}]^2} = \frac{1}{5}$ ,  $i = 1, 2$ ;  $\overline{[C_{ZY}^{(3)}]^2} = \frac{1}{15}$ ;  $\overline{A_{ZY}^{(i)} A_{ZY}^{(j)}} = -\frac{1}{30}$ ,  $i \neq j$ ;  $\overline{B_{ZY}^{(i)} B_{ZY}^{(j)}} = 0$ ,  $i \neq j$ ;  $\overline{C_{ZY}^{(i)} C_{ZY}^{(3)}} = -\frac{1}{10}$ ,  $i = 1, 2$ ;  $\overline{C_{ZY}^{(1)} C_{ZY}^{(2)}} = \frac{1}{10}$ .

---

- [1] J. Heath, S.C. O'Brian, Q. Zhang, Y. Liu, R.F. Curl, H.W. Kroto, F.K. Tittel, and R.E. Smalley, *J. Am. Chem. Soc.* **107**, 7779 (1985).
- [2] M.S. Dresselhaus, G. Dresselhaus, and P.C. Eklund, *Science of Fullerenes and Carbon Nanotubes* (Academic Press, San Diego, 1996).
- [3] H. Shinohara, *Rep. Prog. Phys.* **63**, 843 (2000).
- [4] C.-R. Wang, T. Kai, T. Tomiyama, T. Yoshida, Y. Kobayashi, E. Nishibori, M. Takata, M. Sakata, and H. Shinohara, *Angew. Chem.* **113**, 411 (2001); C.-R. Wang, M. Inakuma, H. Shinohara, *Chem. Phys. Lett.* **300**, 379 (1999).
- [5] P.W. Fowler and D.E. Manolopoulos, *An Atlas of Fullerenes* (Clarendon Press, Oxford, 1995).
- [6] M. Krause, M. Hulman, H. Kuzmany, O. Dubay, G. Kresse, K. Vietze, G. Seifert, C. Wang and H. Shinohara, *Phys. Rev. Lett.* **93**, 137403 (2004).
- [7] G. Kresse and J. Furthmüller, *Comput. Mater. Sci.* **6**, 15 (1996).
- [8] M. Krause, M. Hulman, H. Kuzmany, T.J.S. Dennis, M. Inakuma, and H. Shinohara, *J. Chem. Phys.* **111**, 7976 (1999).
- [9] M. Krause, M. Hulman, H. Kuzmany, P. Kuran, L. Dunsch, T.J.S. Dennis, M. Inakuma, and H. Shinohara, *J. Mol. Struct.* **521**, 325 (2000).
- [10] P.W. Atkins and R.S. Friedman, *Molecular Quantum Mechanics* (Oxford University Press, Oxford, 1997).
- [11] B.J. Berne and R. Pecora, *Dynamic Light Scattering* (John Wiley, New York, 1976).
- [12] T.J.S. Dennis, K. Prassides, E. Roduner, L. Cristofolini, and R. DeRenzi, *J. Phys. Chem.* **97**, 8553 (1993).
- [13] R.M. Mcrae, K. Prassides, I.M. Thomas, E. Roduner, C. Niedermayer, U. Binniger, C. Bernhard, and A. Hofer, *J. Phys. Chem.* **98**, 12133 (1994).
- [14] Y. Maniwa, A. Ohi, K. Mizoguchi, K. Kume, K. Kikuchi, K. Saito, I. Ikemoto, S. Suzuki, and Y.J. Achiba, *J. Phys. Soc. Jpn.* **62**, 1131 (1993).

- [15] R. Blinc, J. Dolinsek, J. Seliger, and D. Arcon, Solid State Commun. **88**, 9 (1993).
- [16] R. Tycko, G. Dabbagh, G.B.M. Vaughan, P.A. Heiney, R.M. Strongin, M.A. Cichy, and A.B. Smith III, J. Chem. Phys. **99**, 7554 (1993).
- [17] C. Christides, T.J.S. Dennis, K. Prassides, R.L. Cappelletti, D.A. Neumann, and J.R.D. Copley, Phys. Rev. B **49**, 2897 (1994).
- [18] M. Yvinec and R.M. Pick, J. Physique **44**, 169 (1983).
- [19] L. Pauling, Phys. Rev. **36**, 430 (1930).
- [20] W. Press, *Single-Particle Rotations in Molecular Crystals*, Springer Tracts Mod. Phys. (Springer Verlag, Berlin, 1981), Vol. 92.
- [21] A. Hüller and D.M. Kroll, J. Chem. Phys. **63**, 4495 (1975).
- [22] See e.g. M. Abramovitz and I.A. Stegun, Editors, *Handbook of Mathematical Functions* (Dover Publications, New York, 1970), p. 721.
- [23] N.W. McLachlan, *Theory and Applications of Mathieu Functions* (Dover Publications, New York, 1964).
- [24] B. De Raedt and K.H. Michel, Phys. Rev. B **19**, 767 (1979).
- [25] P. Debye, *The Collected Papers of Peter J.W. Debye* (Interscience, New York, 1954).
- [26] N.T. Coffey, D.A. Garanin, and D.J. McCarthy, *Advances in Chemical Physics*, **117**, p. 483, Edited by I. Prigogine and Stuart A. Rice (John Wiley, 2001).
- [27] J.R.D. Copley, D. A. Neumann, R.L. Cappelletti, and W.A. Kamitakahara, J. Phys. Chem. Solids **53**.
- [28] C.J. Bradley and A.P. Cracknell, *The Mathematical Theory of Symmetry in Solids* (Clarendon, Oxford, 1972).
- [29] H.A. Kramers, Physica (Utrecht) **7**, 284 (1940).